PHYSICAL REVIEW B VOLUME 37, NUMBER 10 1 APRIL 1988

Model for a glassy adsorbate: Two-level systems and specific heat

Werner Uhler and Rolf Schilling
Institute of Physics, University of Basel, CH-4056 Basel, Switzerland
(Received 17 July 1987)

A two-dimensional Frenkel-Kontorova model with piecewise harmonic substrate potential is used to investigate the properties of a glassy adsorbed layer of atoms interacting via harmonic nearest-neighbor forces. An infinite number of metastable configurations is found. Under certain conditions these are in a one-to-one correspondence to a class of sequences of integers (symbols) in analogy to chaotic dynamical systems also demonstrating the possibility of two-dimensional spatial chaos. A microscopic derivation of the simplest two-level systems is given. Their asymmetries, potential barriers, and density of states are determined analytically. We have found that the density of states depends sensitively on type and degree of the disorder of the adsorbed layer. For quasi-one-dimensional disorder produced by "kink" defects, earlier results for a one-dimensional model are reproduced, leading for the specific heat to a power law $c(T)\sim T^{\tilde{d}}$ with a fractional exponent smaller than 1. On the other hand, for "Gaussian" disorder obtained from an idealized quenched process, we find a constant density of states and therefore a linear specific heat, provided the quenching temperature $T_{\rm qu}$ is sufficiently high. For decreasing $T_{\rm qu}$ the density of states becomes nonconstant, developing structures on any energy scale. Furthermore, we show the time dependence of the specific heat to be exponential.

I. INTRODUCTION

The lack of symmetry of amorphous structures makes theoretical investigation very difficult, and, hence, their microscopic description is a challenge. The utmost interesting problem is whether a system of particles without built-in randomness (i.e., the interactions are invariant under a nontrivial group of translations and rotations) can form glassy configurations. This question is answered by many numerical calculations for a few hundreds of atoms, but a general answer is still desirable.

Recently we followed an approach having its origin in the field of nonlinear dynamical systems. There it was shown that even simple deterministic equations of motion (invariant under time translations) may exhibit rather complex behavior in time; today, this is called temporal chaos. Restricting ourselves to one dimension, we have investigated the possibility of spatial chaos.[1-3] We found a simple, translationally invariant model with anharmonic and competing interactions which exhibits an infinite number of spatially chaotic (glasslike) and metastable configurations. These configurations were shown to exhibit short-range order but no long-range order.[3] One of our major results was a microscopic derivation of configurational excitations forming two-level systems (TLS's). Their contribution to the specific heat below 1 K shows, under certain conditions, a power-law behavior $c(T)\sim T^{\tilde{d}}$ with $\tilde{d}<1$.

For more than a decade such TLS's have been believed to govern the low-temperature properties of amorphous materials in a universal manner. Anderson, Halperin, and Varma[4] and Phillips[5] independently introduced this concept to explain the low-temperature anomalies found by Zeller and Pohl.[6] Assuming a smooth distribution of both energy asymmetries and barrier heights of the TLS's on energy scales relevant at temperatures below 1 K these authors found $\kappa(T)\sim T^2$ for the thermal conductivity, $c(T)\sim T$ for the specific heat, and showed, in addition, that $c(T)$ should depend logarithmically on the time scale of the measurement. However, most experiments show considerable deviations from these predictions. Power laws can be fitted, $c(T)\sim T^{\tilde{d}}$, with a fractional exponent $\tilde{d}$ $(0.5<\tilde{d}<1.3)$ depending on the material, quenching rate, etc.,[7,8] thus implying a nonconstant density of states. This is also experimentally confirmed by phonon-echo experiments of Molenkamp and Wiersma[9] who found, for the density of states, $n(\varepsilon)\sim\varepsilon^{0.3}$. For details of the low-temperature physics of amorphous materials the reader is referred to Ref. 10 and to the reviews by v. Löhneysen[11] and by Hunklinger and Raychaudhuri.[12]

The density of the TLS contributing to the specific heat below 1 K is about 10^{-6} per atom. This makes it almost impossible to calculate $n(\varepsilon)$ (e.g., for a Lennard-Jones system) numerically. Indeed, for 500 particles only four TLS's with energy smaller than 3.4×10^{-4} eV were found.[13] Consequently, simple models like the one-dimensional chain we have studied are helpful. It is the purpose of this paper to extend our recent work to two-dimensional systems where we will focus on the TLS's, their density of states, and the specific heat. For a short review of the present theoretical work concerning TLS's see the introduction of Ref. 3 and the overview given by Hunklinger and Raychaudhuri.[12]

In two dimensions it is most natural to consider an adsorbed monolayer of atoms interacting with a substrate. Such a system already satisfies two necessary conditions for bearing disordered (spatially chaotic) configurations: (i) anharmonicity produced by the substrate and (ii) competition of the interatomic interactions and the interaction between the atoms and the substrate. In order to describe such a monolayer we use a two-dimensional Frenkel-Kontorova model. In a first step the metastable configurations of the model are derived and shown to be spatially chaotic. Then we turn to the investigation of transitions between metastable configurations differing from each other only locally and which we identify with the TLS's in our model. Assuming that the driving mechanism of the transitions is phonon-assisted tunneling, these excitations are shown to be important at even very low temperatures. Their density of states (determining the low-temperature properties of the system) is calculated for two different kinds of disorder.

This paper is organized as follows. In Sec. II we introduce the model and classify its metastable configurations. The TLS, their classical excitation energies (asymmetries) and potential barrier heights will be discussed in Sec. III.

In the subsequent two sections we investigate the corresponding density of states for a quasi-one-dimensional disorder with "kink defects" (Sec. IV) and for two-dimensional, "Gaussian" disorder obtained from a quench process (Sec. V). Finally, Sec. VI contains a summary and discussion of our results.

II. MODEL

We consider a layer of adsorbed atoms which topologically form a square lattice; i.e., the "bonds" of the atoms build four-sided cells and each atom has exactly four neighbors. The adsorbed atoms interact harmonically with their neighbors and, in addition, with a periodic substrate potential. The substrate is assumed to be a square lattice with lattice constant a (Fig. 1). This model is just a two-dimensional Frenkel-Kontorova (FK) model.[14] If the substrate potential is much stronger than the nearest-neighbor interaction it can well be approximated by a piecewise parabolic potential (Fig. 2). Hence, the following system with the potential energy

$$V(\mathbf{x})=\frac{C}{4}\sum_{\mathbf{j},\boldsymbol{\delta}}[\mathbf{x}(\mathbf{j}+\boldsymbol{\delta})-\mathbf{x}(\mathbf{j})-a\boldsymbol{\mu}_{\boldsymbol{\delta}}]^2 + \frac{\lambda C}{2}\sum_{\mathbf{j}}[\mathbf{x}(\mathbf{j})-a\mathbf{m}(\mathbf{j};\mathbf{x})]^2 \tag{1a}$$

with the "cell" variable (cf. Fig. 1)

$$m^{\alpha}(\mathbf{j};x^{\alpha})=\operatorname{int}[x^{\alpha}(\mathbf{j})/a+\tfrac{1}{2}] \quad (\alpha=1,2) \tag{1b}$$

will be investigated. The first term accounts for the nearest-neighbor interactions, with $C>0$ the corresponding coupling constant, and the substrate potential with relative strength $\lambda>0$ is represented by the second term. The integer double index $\mathbf{j}=(j_1,j_2)$, which labels the atoms, has a range $j_\alpha=0,1,\ldots,N_\alpha-1$, so that the system consists of $N=N_1N_2$ particles. The index $\boldsymbol{\delta}$ runs over all nearest-neighbor vectors of a square lattice, a $\boldsymbol{\mu}_{\boldsymbol{\delta}}$ is the equilibrium position of the nearest-neighbor bonds. $\mathbf{x}$ always stands for the whole set of positions $\{\mathbf{x}(\mathbf{j})\}$. The one-dimensional version of this model has been studied extensively by several authors.[15,16]

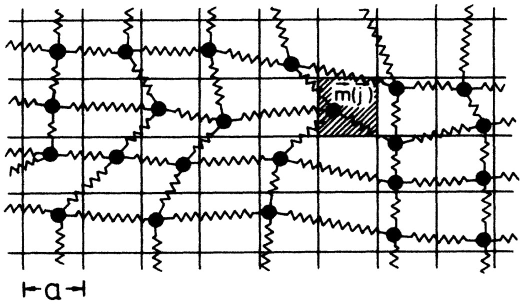

FIG. 1. Top view of a part of the adsorbed layer. The hatched region indicates the "cell" $\mathbf{m}(\mathbf{j})$ the particle $\mathbf{j}$ is sitting in, and a is the period of the substrate.

The stationary configurations $\mathbf{x}_0$ of our system [with potential energy (1)] are solutions of $\delta V/\delta x^{\alpha}=0$, i.e., solutions of the nonlinear difference equation

$$(D_\lambda x_0^\alpha)(\mathbf{j})=-\sum_{\boldsymbol{\delta}}[x_0^\alpha(\mathbf{j}+\boldsymbol{\delta})-x_0^\alpha(\mathbf{j})]+\lambda x_0^\alpha(\mathbf{j})] = \phi(\mathbf{j};x_0^\alpha)\ , \tag{2a}$$

with the nonlinearity

$$\phi(\mathbf{j};x_0^\alpha)=\lambda a m^{\alpha}(\mathbf{j};x_0^\alpha)\ . \tag{2b}$$

The operator D_λ is related to the discrete Laplacian Δ by

$$D_\lambda=-\Delta+\lambda\ . \tag{3}$$

Let $g_\lambda(\mathbf{j})$ denote the Green's function of D_λ: i.e.,

$$(D_\lambda g_\lambda)(\mathbf{j})=\delta_{\mathbf{j},0}\ . \tag{4}$$

An explicit representation and properties of $g_\lambda(\mathbf{j})$, which we will use in the following, are given in Appendix A.

Noticing that the difference equation (2) does not couple the components of α of $\mathbf{x}$, we will suppress α in the following except where it is necessary. Splitting up $x(\mathbf{j})$ into a "cell position" and "intracell position,"

$$x(\mathbf{j})=am(\mathbf{j};x)+u(\mathbf{j})\ , \tag{5}$$

we can rewrite the difference equation as

$$D_\lambda u_0(\mathbf{j})=a\Delta m(\mathbf{j};x_0)\ . \tag{6}$$

Using the Green's function this is equivalent to

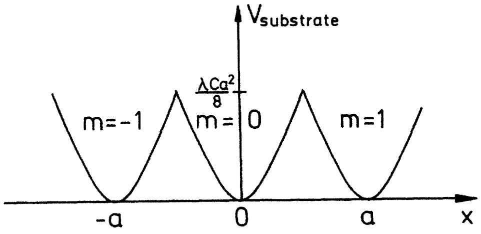

FIG. 2. The substrate potential along the x axis. The integers m (1 component) of the "cells" are indicated.

$$x_0(\mathbf{j})=am(\mathbf{j};x_0)+a\sum_{\mathbf{k}}g_\lambda(\mathbf{j}-\mathbf{k})\Delta m(\mathbf{k};x_0)\ . \tag{7}$$

Equation (7) is nothing more than the "integral equation" associated with Eq. (2). However, suppose for a moment that $m(\mathbf{k};x_0)$ would not depend on $\{x_0(\mathbf{k})\}$. Then specifying an arbitrary set of integers $m=\{m(\mathbf{k})\}$, Eq. (7) determines a configuration

$$x_0(m)\equiv\{x_0(\mathbf{j};m)\} \tag{8}$$

of the adsorbed atoms. But Eq. (1b) readily shows that this is a solution of the difference equation if and only if the self-consistency condition (SCC)

$$m(\mathbf{j})=\operatorname{int}[x_0(\mathbf{j};m)/a+\tfrac{1}{2}] \tag{9}$$

is satisfied. This restricts the possible integer configurations $\{m(\mathbf{k})\}$. Using (7), Eq. (9) can be written in a more suitable form

$$\left|\sum_{\mathbf{k}}g_\lambda(\mathbf{j}-\mathbf{k})\Delta m(\mathbf{k})\right|<\tfrac{1}{2}\quad\forall\mathbf{j} \tag{10}$$

with the physical meaning that the moduli of the intracell positions must not exceed $a/2$, as also required by their definition. It is obvious that any crystalline "integer configuration," i.e.,

$$m(\mathbf{k})=\mathbf{a}\cdot\mathbf{k}+m(0)$$

with an arbitrary integer-valued vector $\mathbf{a}$, will satisfy the self-consistency condition. Before discussing (10) we introduce bond variables via

$$\sigma(\mathbf{j})=\nabla m(\mathbf{j})\ . \tag{11}$$

Here the discrete gradient operator ∇ is defined by the partial difference operators

$$d_\alpha x(\mathbf{j})=x(\mathbf{j}+\mathbf{e}_\alpha)-x(\mathbf{j})\quad(\alpha=1,2) \tag{12a}$$

($\mathbf{e}_\alpha$ are the canonical unit vectors in two dimensions) such that

$$\nabla x(\mathbf{j})=[d_1x(\mathbf{j})]\mathbf{e}_1+[d_2x(\mathbf{j})]\mathbf{e}_2\ . \tag{12b}$$

For later purposes (in Sec. V) we already introduce here conjugate operators

$$d_\alpha^\dagger x(\mathbf{j})=x(\mathbf{j}-\mathbf{e}_\alpha)-x(\mathbf{j})\quad(\alpha=1,2) \tag{12c}$$

(conjugate with respect to the scalar product introduced in Sec. V) and discrete divergence and rotation

$$\operatorname{div}\mathbf{y}(\mathbf{j})=-\nabla^\dagger\cdot\mathbf{y}(\mathbf{j})\ ,$$

$$\operatorname{rot}\mathbf{y}(\mathbf{j})=\nabla\cdot\overleftrightarrow{\varepsilon}\cdot\mathbf{y}(\mathbf{j})\ , \tag{12d}$$

where $\overleftrightarrow{\varepsilon}$ is the totally antisymmetric tensor in two dimensions. The discrete Laplacian can be written as

$$\Delta x(\mathbf{j})=-\nabla^\dagger\cdot\nabla x(\mathbf{j})\ . \tag{12e}$$

Now let us turn back to the SCC (10). For noncrystalline configurations the fluctuations of the σ's around their mean value

$$\mathbf{l}=N^{-1}\sum_{\mathbf{j}}\sigma(\mathbf{j}) \tag{13}$$

will deviate from zero leading to a competition between elastic and substrate interaction of the adsorbed layer. In order that the SCC holds, these fluctuations must be bounded by a value r depending on the relative strength of the substrate potential, i.e.,

$$|[\sigma(\mathbf{j})-\mathbf{l}]\cdot\mathbf{e}_\alpha|\le r \tag{14}$$

for all $\mathbf{j}$ and all $\mathbf{e}_\alpha$.

To be more precise: For a given r (characterizing the degree of disorder) a $\lambda_c(r)$ can be found such that all configurations obeying Eq. (14) also fulfill the SCC provided $\lambda>\lambda_c(r)$. Moreover, in this case it can be shown that all stationary solutions $\{x_0(\mathbf{j})\}$ with bounded fluctuations of the bond lengths can be uniquely labeled by "sequences of symbols" $\{\sigma(\mathbf{j})\}$ satisfying Eq. (14). A lemma stating this fact in detail, and its proof, is given in Appendix B.

With this result we reobtain the context of dynamical systems. Equation (2) can be regarded as the evolution equation of a dynamical system with two discrete "times" j_1 and j_2. But, the evolution in one "time" variable is not independent of the other. In fact, the condition

$$\operatorname{rot}\sigma(\mathbf{j})=0 \tag{15}$$

(a consequence of the definition of the σ's as a gradient field) assures that going from time $t=(j_1,j_2)$ to time $t'=(j_1',j_2')$ is independent of the path in time space. Now, the classification of the solutions of Eq. (2) by sequences of symbols corresponds to the well-known symbolic dynamics. We have much freedom in choosing our sequences of symbols; the only restrictions stem from Eqs. (14) and (15). But Eq. (15) cannot be regarded as a "proper" restriction because it naturally arises in dynamical systems with more than one time coordinate in order to ensure the "path independence" of the evolution. Thus the equivalence of solutions of (2) and sequences of symbols can be considered as an embedding of a generalized Bernoulli shift.[17] Therefore, we feel justified to call our system spatially chaotic. Physically speaking, the freedom in selecting the σ shows the existence of spatially disordered stationary solutions. These integer (symbolic) variables describe the "quenched" disorder of the glassy adsorbed layer.

The metastability of a stationary configuration $\{x_0(\mathbf{j})\}$ is easily shown by expanding the energy around x_0. The dynamical matrix can be diagonalized yielding for the phonon frequencies

$$\omega(\mathbf{q})=\omega_g[1+2(2-\cos q_1-\cos q_2)/\lambda]^{1/2}\ , \tag{16a}$$

$$\omega_g=(\lambda C/m)^{1/2}\ , \tag{16b}$$

where m is the mass of the adsorbed atoms. Since $\omega(\mathbf{q})$ is always larger than or equal to the gap frequency ω_g, all stationary configurations are locally stable. That the dispersion (16) is independent of $\{x_0(\mathbf{j})\}$ is related to the substrate potential being piecewise harmonic. Thus, for our model we have managed to separate the configurational degrees of freedom described uniquely by $\{\sigma(\mathbf{j})\}$ and the vibrational part. The latter can be neglected at temperatures much smaller than the phonon gap ω_g.

The energy of a metastable configuration is calculated by substituting Eq. (7) [with given $\{m(\mathbf{k})\}$] into Eq. (1a), which on using Appendix A finally yields the expression

$$V(\mathbf{x}_0)=E(\sigma^1,\sigma^2)=\sum_{\alpha=1,2}E(\sigma^2)$$
$$=(Ca^2/2)\sum_{\alpha=1,2}\left[\sum_{\mathbf{j},\mathbf{k}}[\sigma^\alpha(\mathbf{j})\cdot\sigma^\alpha(\mathbf{k})\delta_{\mathbf{j},\mathbf{k}}-\operatorname{div}\sigma^\alpha(\mathbf{j})g_\lambda(\mathbf{j}-\mathbf{k})\operatorname{div}\sigma^\alpha(\mathbf{k})]-2\sum_{\mathbf{j}}\sigma^\alpha(\mathbf{j})\cdot\mu^\alpha+N\mu^{\alpha^2}\right], \tag{17}$$

where

$$\sigma^\alpha(\mathbf{j})=\nabla m^\alpha(\mathbf{j}) \tag{18a}$$

and

$$\mu^\alpha=(\mathbf{e}_\alpha\cdot\mu_{\mathbf{e}_1})\mathbf{e}_1+(\mathbf{e}_\alpha\cdot\mu_{\mathbf{e}_2})\mathbf{e}_2 . \tag{18b}$$

Of course, the ground state will depend on μ_δ and may exhibit a number of interesting properties such as incommensurability effects which were found for the corresponding one-dimensional model.[15,16] As we do not investigate ground-state properties, we believe these effects to be of no importance for our disordered configurations. Consequently we choose μ_δ integer valued so that the ground state is always given by $\sigma^\alpha(\mathbf{j})=\mu^\alpha$ for all $\mathbf{j}$.

III. TWO-LEVEL SYSTEMS

In this section the TLS's will be investigated. In Sec. II we showed that the adsorbed layer can be in one of many locally stable states, their number increasing exponentially with N. The potential-energy landscape in configuration space is complex, and it will occur that the energy difference between two adjacent valleys (corresponding to two configurations differing from each other only locally) can become arbitrarily small.

In the following we consider the simplest type of TLS where one particle jumps into one of its four nearest-neighbor cells (as is shown in Fig. 3) and the system is allowed to relax afterwards. This kind of configurational excitation was first studied by Pietronero and Strässsler[16] for the corresponding one-dimensional model with a fixed ratio ζ of the mean distance of the particles to the period a. The contribution to the low-temperature specific heat for the system at equilibrium was discussed in Ref. 18. A Schottky-type behavior with strong incommensurability effects (because ζ was not an integer) was found.[19] The present work is different from that in Refs. 16, 18, and 19 in two respect: first, we consider configurations with frozen-in disorder corresponding to nonequilibrium configurations which are insensitive on ζ and, second, our system is two dimensional.

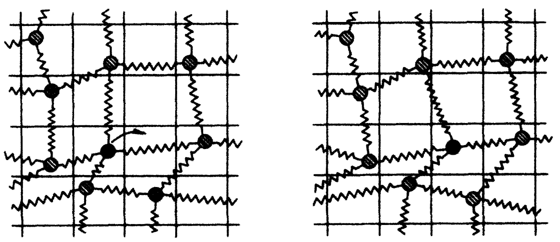

FIG. 3. A configurational excitation forming a TLS: The black particle moves into a neighboring cell.

A. Asymmetries

The type of TLS described above can be represented by a transition between two metastable configurations represented by $\{\mathbf{m}(\mathbf{k})\}$ and $\{\mathbf{m}'(\mathbf{k})\}$ for which

$$\mathbf{m}'(\mathbf{k})=\mathbf{m}(\mathbf{k}) \quad \text{for all } \mathbf{k}\neq\mathbf{j}_0 ,$$
$$\mathbf{m}'(\mathbf{j}_0)=\mathbf{m}(\mathbf{j}_0)+\mathbf{e} , \tag{19}$$

where $\mathbf{e}$ is one of the four nearest-neighbor vectors of the "substrate lattice" (Fig. 3). Without loss of generality we choose $\mathbf{e}=\mathbf{e}_1$. Then the asymmetry ε (cf. Fig. 4) will only depend on $\{m^1(\mathbf{j})\}$ (the superscript $\alpha=1$ is suppressed again). With Eqs. (17) and (19) we find for ε

$$\varepsilon(\mathbf{j}_0;m)=E(m')-E(m)$$
$$=\varepsilon_0-\lambda Ca^2\sum_{\mathbf{k}}g_\lambda(\mathbf{j}_0-\mathbf{k})\Delta m(\mathbf{k}) , \tag{20a}$$

where

$$\varepsilon_0=-(\lambda Ca^2/2)\Delta g_\lambda(0)>0 . \tag{20b}$$

[$E(m)$ follows from (17) by substituting (18a).] Clearly, $\varepsilon(\mathbf{j}_0;m)$ depends on $\{m(\mathbf{k})\}$. For a crystalline arrangement of the atoms this yields

$$\varepsilon(\mathbf{j}_0;m_{\text{cryst}})=\varepsilon_0 \tag{21}$$

for all $\mathbf{j}_0$. A broad distribution of ε only results if the configuration $\{m(\mathbf{k})\}$ is irregular which, in turn, induces a broad distribution of the intracell positions $u(\mathbf{j})$ of the atoms. It is interesting to note that this close relationship between ε and $u(\mathbf{j})$ can be made explicit for our model:

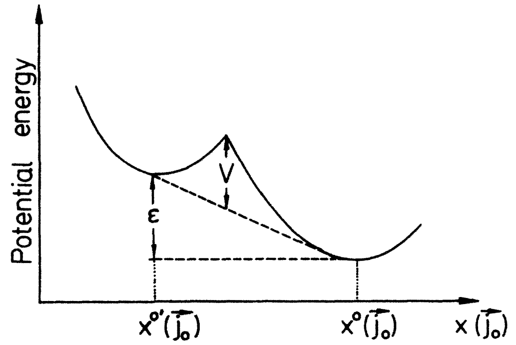

FIG. 4. The potential energy of the system during the motion of the particle $\mathbf{j}_0$ between the equilibrium positions $x_0(\mathbf{j}_0)$ and $x_0'(\mathbf{j}_0)$ in neighboring cells. ε and V denote energy asymmetry and potential barrier, respectively.

$$\varepsilon(\mathbf{j}_0;m)=\varepsilon_0-\lambda C a u_0(\mathbf{j}_0;m) \tag{22}$$

following from Eqs. (5), (7), and (20). Because $u_0(\mathbf{j};m)$ is bounded for all $\mathbf{j}$ due to the self-consistency condition, the spectrum of the asymmetries must be bounded as well:

$$\varepsilon_0-\lambda C a^2/2 \leq \varepsilon(\mathbf{j}_0;m) \leq \varepsilon_0+\lambda C a^2/2 \ . \tag{23}$$

The density of states $n(\varepsilon)$ will be discussed in Secs. IV and V.

B. Potential barriers

Now we turn to the calculation of the potential barriers V separating the local minima of our TLS (cf. Fig. 4). V is obtained from the work done by an external force F acting on particle $\mathbf{j}_0$ in order to change the configuration $\{m(\mathbf{k})\}$ into $\{m'(\mathbf{k})\}$. This induces in Eq. (1) an extra term $-x(\mathbf{j}_0)F$ changing the difference equation (2a) into

$$(D_\lambda x_0)(\mathbf{j})-\phi(\mathbf{j};x_0)=(F/C)\delta_{\mathbf{j},\mathbf{j}_0} \ . \tag{24}$$

Inserting the ansatz

$$x_0(F,\mathbf{j})=x_0(\mathbf{j})+w(F,\mathbf{j}) \tag{25}$$

for the solution $x_0(F,\mathbf{j})$ into (24) we obtain for w the inhomogeneous linear equation

$$(D_\lambda w)(F,\mathbf{j})=(F/C)\delta_{\mathbf{j},\mathbf{j}_0} \tag{26}$$

with the solution

$$w(F,\mathbf{j})=(F/C)g_\lambda(\mathbf{j}-\mathbf{j}_0) \ . \tag{27}$$

Here (A1) was used. Noticing that (19) only affects one spatial component of the atomic positions, the work done by the external force can be obtained by integrating Eq. (27) from the equilibrium position $x_0(\mathbf{j})$ to the border of the cell. The potential barrier is defined as the mean value of the work required in each of the two cells (cf. Fig. 4) which finally yields

$$\begin{aligned} V(\mathbf{j}_0;m)=[Ca^2/2g_\lambda(0)]\{&[\tfrac{1}{2}-u_0(\mathbf{j}_0;m)/a]^2 \\ &-\lambda g_\lambda(0)[\tfrac{1}{2}-u_0(\mathbf{j}_0;m)/a] \\ &+[\lambda g_\lambda(0)]^2/2\} \ . \end{aligned} \tag{28}$$

Since $u_0(\mathbf{j}_0,m)$ is bounded there exist lower and upper bounds for V, $V_{\min}$, and $V_{\max}$, respectively, quite similar to the results for the one-dimensional model.[3] Using the self-consistency condition and Eq. (A5) we find

$$V_{\min}(\lambda) \geq V_0=\lambda^2(Ca^2/8)g_\lambda(0) \ , \tag{29a}$$

$$V_{\max}(\lambda) \leq \lambda(Ca^2/2)\{1+[1-\lambda g_\lambda(0)]^2\}/[2\lambda g_\lambda(0)] \ . \tag{29b}$$

V_0 is reduced by a positive factor $\lambda g_\lambda(0)<1$ with respect to the "naked" barrier $(\lambda Ca^2)/8$ due to the nearest-neighbor interaction. This has already been observed by Beyeler *et al.*[18] for the one-dimensional Frenkel-Kontorova model.

C. Correlations between asymmetries and barrier heights

Correlations between asymmetries and potential barriers have been shown to be important for the time dependence of the specific heat by Phillips.[5] We will show here that for our model the asymmetry completely determines the potential barrier (and vice versa) and we discuss the time dependence of the specific heat originating from this fact.

Inserting (22) into (28) yields

$$V=V_0[1+(\varepsilon/4V_0)^2] \tag{30}$$

confirming the dependence of $V(\mathbf{j}_0;m)$ on $\varepsilon(\mathbf{j}_0;m)$. Moreover, from (30) it becomes clear that for TLS contributing to the specific heat at about 0.1–1 K (asymmetries of the order 10^{-5}–10^{-4} eV) the potential barriers are almost fixed. This can be seen as follows: The potential barrier produced by the substrate alone is assumed to be of the order of 0.1 eV, and $\lambda g_\lambda(0)\approx 0.7$ for $\lambda=10$, which is a reasonable value for the ratio of substrate interaction to nearest-neighbor interaction of strongly adsorbed particles.[20] From this, Eq. (29a), and Eq. (30), we find that the relative variation of V induced by ε (in the appropriate range) is 10^{-6}–10^{-8} and can therefore be neglected.

Discussing the time dependence of the specific heat we will closely follow the concepts given by Jäckle.[21] Application of this theory can be justified by the following considerations: At low temperatures, transitions between the two states of our TLS will only occur by phonon-assisted tunneling. But the phonons of the adsorbate possess a gap with frequency $\omega_g=(\lambda C/m)^{1/2}$. Assuming m to be the mass of an oxygen atom, the lattice constant a to be 2 Å, and V_0 to be 0.1 eV, we find the temperature corresponding to the gap to be about 145 K. Therefore, these phonons cannot contribute to the phonon-assisted tunneling far below this temperature. This can only be achieved by the phonons of the substrate. Following Jäckle we assume that the TLS couple via a deformation potential to the local strains of the substrate. Thus the results of Ref. 21 are valid with only slight modifications.

Let us now turn to some more detailed investigations. Allowing transitions with coupling $\Delta/2$ between both states of a TLS we obtain, for the energy splitting E,

$$E=\pm(\varepsilon^2+\Delta^2)^{1/2} \ , \tag{31}$$

where ε is the classical energy difference (asymmetry).[22] (The sign of E is determined by the sign of ε.) A simple Wentzel-Kramers-Brillouin (WKB) expression for Δ is[4]

$$\Delta=\hbar\omega_0 e^{-\Lambda} \tag{32}$$

with the tunneling parameter[23]

$$\Lambda=\tfrac{1}{2}(2mV/\hbar^2)^{1/2}l \ . \tag{33}$$

Here $\hbar\omega_0$ is the zero-point energy, V is the barrier height, and l is the tunneling distance. The relaxation rate is then given by[21]

$$\tau^{-1}(E,\Delta)=(\tau^{-1})_{\max}(E)(\Delta/E)^2 \tag{34a}$$

with the maximum rate

$$(\tau^{-1})_{\max}(E)=(1/c_l^5+2/c_t^5)[B^2/6\pi\rho\hbar^4] \times E^3\coth(\beta E/2) , \tag{34b}$$

where c_l and c_t are longitudinal and transverse sound velocities of the substrate, B is its deformation potential, and ρ is its density. The geometrical restrictions arising from the fact that the TLS are sitting at the surface have been accounted for by a factor $\frac{1}{3}$ compared to the results of Jäckle.[24] (As we are only interested in the order of magnitude of the relaxation time, the exact value of this factor is irrelevant.)

In order to calculate the time-dependent specific heat given by

$$C(T,t)=k_B\int_0^\infty dE\int_0^1 dr\,P(E,r)f(\beta E) \times\{1-\exp[-t/\tau(E,r)]\} , \tag{35}$$

where

$$f(x)=x^2\exp(-x)/[1+\exp(-x)]^2 , \tag{36}$$

we need the distribution function $P(E,r)$. Here we have introduced $r=(\Delta/E)^2$ as a new variable. Inserting (30) into (33) we get, for $\varepsilon/V_0 \ll 1$,

$$\Lambda=\Lambda_0[1+(\varepsilon/4V_0)^2] \tag{37a}$$

with

$$\Lambda_0=\tfrac{1}{2}(2mV_0/\hbar^2)^{1/2}l . \tag{37b}$$

For small ε this immediately leads to

$$\Delta(\varepsilon)=\Delta_0\exp[-(\Lambda_0/2)(\varepsilon/4V_0)^2] , \tag{38a}$$

where

$$\Delta_0=\hbar\omega_0 e^{-\Lambda_0} . \tag{38b}$$

From the joint distribution of ε and Δ,

$$P(\varepsilon,\Delta)=n(\varepsilon)\delta(\Delta-\Delta(\varepsilon)) , \tag{39}$$

the distribution of E and r can be obtained in a straightforward manner:

$$P(E,r)=n[(1-r)^{1/2}E]\,|E|\,[4r(1-r)]^{-1/2}\delta(r^{1/2}|E|-\Delta_0\exp[-(\Lambda_0/2)(1-r)(E/4V_0)^2]) . \tag{40}$$

Noticing that $(E/4V_0)^2<10^{-6}$ for $E<10^{-4}$ eV, P can well be approximated by

$$P(E,r)\approx(1-r)^{-1/2}n[(1-r)^{1/2}E] \times\delta(r-(\Delta_0/E)^2) . \tag{41}$$

Substituting this in Eq. (35) and taking into account that f has a relatively sharp maximum at $x_{\max}\approx 2.4$ it follows that

$$C(T,t)\approx C(T,\infty)\{1-\exp[-t/\tau(T)]\} , \tag{42a}$$

where

$$C(T,\infty)=k_B\int_0^\infty n(E)f(\beta E)\,dE , \tag{42b}$$

$$\tau^{-1}(T)=k_BT(1/c_l^5+2/c_t^5)[B^2\Delta_0^2/(6\pi\rho\hbar^4)] \times x_{\max}\coth(x_{\max}/2) . \tag{42c}$$

Thus we find an exponential time dependence with a temperature-dependent relaxation time which is of the order of 10^{-3} s up to several seconds (depending on the parameter values of the system) for temperatures between 0.1 and 1 K. The exponential behavior is due to the very sharp distribution of the barrier heights for TLS with asymmetry below 10^{-4} eV. This sharp distribution is typical for the model of an adsorbed layer in a strong substrate potential. The reader should also note that the long-time specific heat [Eq. (42b)] is completely determined by the distribution function $n(\varepsilon)$ of the asymmetries.

IV. QUASI-ONE-DIMENSIONAL DISORDER: DENSITY OF STATES

In Sec. III we have calculated the asymmetry ε and the corresponding barrier height V for the simplest type of

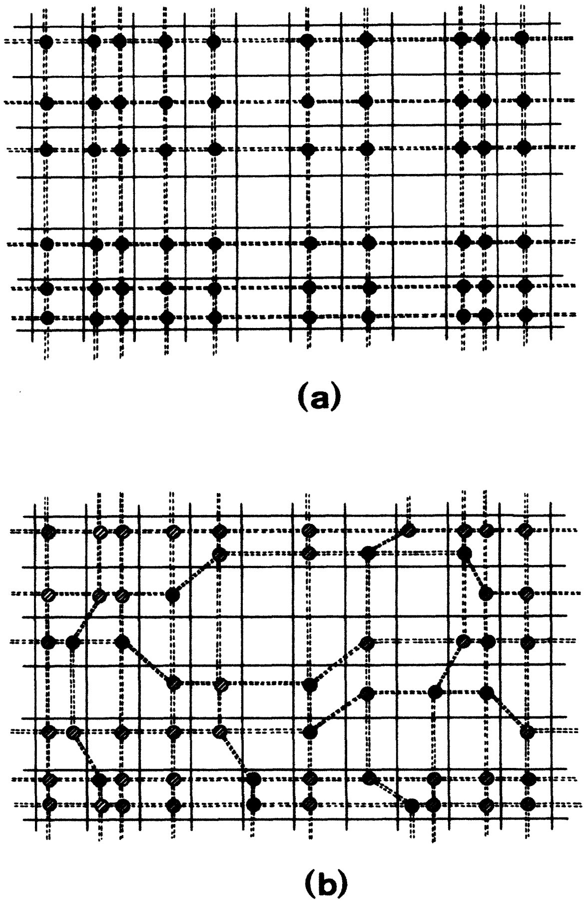

FIG. 5. A quasi-one-dimensionally disordered system: (a) without, and (b) with "kink defects" represented by the solid circles.

TLS where only one atom is moved into one of its adjacent cells. It was found that ε and V are strongly correlated [cf. Eq. (30)] and depend on the quenched variables $\{m(\mathbf{k})\}$. Primarily, we are interested in the density of states. By an argument completely analogous to that given in Ref. 3 it can be shown that (choosing the same parameter values as in Sec. III) quantum corrections can be neglected for energies $E \gg \Delta_0 \approx 10^{-9}$ eV. Thus, the density of states is well approximated by the distribution of the asymmetries.

Now, determining $n(\varepsilon)$ requires a distribution function $\rho(\{m(\mathbf{k})\})$ [or equivalently $\rho(\{\sigma(\mathbf{k})\})$] which characterizes the quenched disorder described by the symbols $\{m(\mathbf{k})\}$ [or $\{\sigma(\mathbf{k})\}$].[25] $n(\varepsilon)$ then follows from[26]

$$n(\varepsilon)=\sum_{m}\delta(\varepsilon-\varepsilon(\mathbf{j}_0;m))\rho(m)\ . \tag{43}$$

In this section we consider a special type of disorder where ρ is of a simple form.

Let us start from configurations $\{m(\mathbf{k})\}$ which are one-dimensionally disordered [Fig. 5(a)]. They are represented by two independent sets of integers $\{\hat{m}^{\,1}(k_1)\}$ and $\{\hat{m}^{\,2}(k_2)\}$ such that

$$m^{\alpha}(\mathbf{k})=\hat{m}^{\,\alpha}(k_\alpha) \tag{44}$$

for all $\mathbf{k}$. Then we introduce kink defects into the rows and columns [Fig. 5(b)]. These are no proper topological defects because the adsorbate is always topologically equivalent to a square lattice. Still, they are commonly used to describe defects in solids.[27]

For simplicity we restrict ourselves to the following configurations satisfying

$$\sigma^{\alpha}(\mathbf{k})=m^{\alpha}(\mathbf{k}+\mathbf{e}_\alpha)-m^{\alpha}(\mathbf{k})\in\{n,n+1\} \tag{45}$$

with n a positive integer. Denoting by $\mathbf{p}$ and $\mathbf{q}$ the positions of the defects in the columns and the rows, respectively, the configuration is given by

$$\begin{aligned} m^{1}(\mathbf{k})&=\hat{m}^{\,1}(k_1)+\sum_{n_2=0}^{k_2-1}\sum_{\mathbf{p}}\delta_{k_1,p_1}\delta_{n_2,p_2}\tau^{1}(\mathbf{p})\ ,\\ m^{2}(\mathbf{k})&=\hat{m}^{\,2}(k_2)+\sum_{n_1=0}^{k_1-1}\sum_{\mathbf{q}}\delta_{n_1,q_1}\delta_{k_2,q_2}\tau^{2}(\mathbf{q})\ . \end{aligned} \tag{46}$$

Here the "kink charges" $\tau^1(\mathbf{p})$ and $\tau^2(\mathbf{q})$ take values -1 and $+1$ with the only restriction being that the configuration (46) has to be compatible with (45) (e.g., the charges must alternate along the columns and rows).

The low-lying excitations are those where the tunneling particle has similar environments in both wells. This is exactly the case for particles sitting at the defects. Consequently, we have to regard transitions where a kink just moves a lattice spacing. Choosing $\mathbf{j}_0=\mathbf{p}_0$ and $\alpha=1$ (without loss of generality) we get, from (20) and (46) after lengthy but straightforward calculations in the thermodynamic limit,[28]

$$\begin{aligned}\varepsilon(\mathbf{p}_0;m)={}&\tau^{1}(\mathbf{p}_0)Ca^{2}[(1-\eta)^{2}/(1+\eta)]\sum_{i_1=1}^{\infty}\eta^{i}[\sigma^{1}(p_{0,1}-i_1-1,p_{0,2})-\sigma^{1}(p_{0,1}+i_1,p_{0,2})]\\ &-\lambda Ca^{2}\sum_{\mathbf{p}\neq\mathbf{p}_0}\tau^{1}(\mathbf{p}_0)\tau^{1}(\mathbf{p})\sum_{i_2=p_2+1}^{\infty}\lambda g_{\lambda}(p_1-p_{0,1},i_2-p_{0,2})\ ,\end{aligned} \tag{47a}$$

where the one-dimensional version (A8) of the Green's function was used and where

$$\eta=1+\lambda/2-[(\lambda/2)^2+\lambda]^{1/2}\ . \tag{47b}$$

According to the restriction (45) the σ^1 variables only take the values n and $n+1$. The first term of (47a) coincides exactly with the asymmetry of the TLS obtained in Refs. 2 and 3 for a chain of particles with anharmonic and competing interactions (except that there the σ variables take values ± 1). The second term describes the interaction of the tunneling particle with other defects. For low defect density, i.e., large distances between the defects, this term becomes negligible. This can be easily seen using the asymptotic form following from (A12):

$$\sum_{i_2=p_2+1}^{\infty}\lambda g_{\lambda}(p_1-p_{0,1},i_2-p_{0,2})\le\frac{\lambda/2}{1-\zeta}(\lambda^2/4+2\lambda)^{-1/2}\zeta^{|p_1-p_{0,1}|+|p_2-p_{0,2}|+1}\ , \tag{48a}$$

where

$$\zeta=[1+\lambda/4+\tfrac{1}{2}(\lambda^2/4+2\lambda)^{1/2}]^{-1}\ . \tag{48b}$$

Taking the parameter values of Sec. III we find from (48) that the defect interaction term can be neglected on an energy scale of 10^{-5} eV provided the minimum distance of the defects is of the order of 10 lattice constants.

From the range of the σ variables [cf. (45)], it can be read off that we must have $\lambda>\lambda_c(\frac{1}{2})$ in order to ensure that SCC is fulfilled. Using the upper bound for $\lambda_c(\frac{1}{2})$ derived in Appendix B, we find from (47b) $\eta\approx 0.16$, which is smaller than $\frac{1}{3}$. ($\eta=\frac{1}{3}$ is equivalent to $\lambda=\frac{4}{3}$.) Therefore, the scaling property found in Refs. 2 and 3 holds (if we use a distribution of the σ's similar to the one used by these authors) finally leading to an approximate[29] power-law behavior for the specific heat

$$c(T) \sim T^{\tilde{d}} \tag{49a}$$

with

$$\tilde{d} = \ln[p^2 + (1-p)^2]/\ln\eta\ , \tag{49b}$$

where p is the probability that $\sigma^1(\mathbf{j}) = n$. For details the reader is referred to Ref. 3.

V. GAUSSIAN DISORDER: DENSITY OF STATES

The type of disorder we have considered in Sec. IV, although not implausible, was introduced in a more or less phenomenological way. A realistic determination of the disorder in a glassy state should start with the fluid phase and subject it to a cooling process. For large enough cooling rates the system will relax into one of the metastable glassy configurations. Unfortunately, the theoretical description of such a glass transition on a microscopic level is still beyond a possible analytical treatment. Consequently, an idealization is necessary.

Starting with the fluid phase, all kinetic energy is taken instantly out of the system at a time t_0. We then assume that during this quenching process the particles just fall into those cells $m(\mathbf{j})$ where they were sitting at t_0 and finally reach the metastable positions $x_0(\mathbf{j};m)$. This is nothing else but a relaxation along the gradient of the potential energy. The simplification is twofold: (i) an infinitely large cooling rate is required, and (ii) it is assumed that the particles will stick to their corresponding cells. The vapor deposition of atoms on a substrate at 4 K, or at even lower temperatures, is a good realization of an almost infinite cooling rate apart from the fact that the atoms will not stick immediately but will migrate, thereby dissipating their binding energy to the substrate. However, we believe our idealization to be instructive.

So we start with the adsorbed layer at high temperatures. The statistical weight of a configuration $\{\mathbf{x}(\mathbf{j})\} = \mathbf{x}$ is given by the canonical ensemble

$$\begin{aligned} \rho(\mathbf{x}) &= Z^{-1}(\beta)\exp[-\beta V(\mathbf{x})]\ , \\ Z(\beta) &= \int \prod_{\mathbf{j}} d^2\mathbf{x}(\mathbf{j})\exp[-\beta V(\mathbf{x})]\ , \end{aligned} \tag{50}$$

with the potential energy V of Eq. (1). The reduced distribution function $\rho_{\text{qu}}(\mathbf{m})$ describing the frozen-in disorder follows from (50) by integrating over the intracell positions $\mathbf{u}(\mathbf{j})$ defined by Eq. (5):[30]

$$\begin{aligned} \rho_{\text{qu}}(\mathbf{m}) &= Z_{\text{qu}}^{-1}(\beta_{\text{qu}}) \int \prod_{\mathbf{j}} d^2\mathbf{u}(\mathbf{j})\exp[-\beta_{\text{qu}} V(a\mathbf{m}+\mathbf{u})]\ , \\ Z_{\text{qu}}(\beta_{\text{qu}}) &= \sum_{\mathbf{m}} \int \prod_{\mathbf{j}} d^2\mathbf{u}(\mathbf{j})\exp[-\beta_{\text{qu}} V(a\mathbf{m}+\mathbf{u})] \\ &= Z(\beta_{\text{qu}})\ . \end{aligned} \tag{51}$$

The integration range is $-a/2 \le u^\alpha(\mathbf{j}) \le a/2$ ($\alpha = 1,2$), $\beta_{\text{qu}} = 1/k_B T_{\text{qu}}$, and T_{qu} is the initial temperature of the fluid when the quenching process starts. The integration in (51) can be carried out exactly up to terms of the order $(\beta_{\text{qu}} C a^2/2)^2$. In the limit for high "quenching temperatures" T_{qu}, i.e., $\beta_{\text{qu}} C a^2/2 \ll 1$, we thus find the following result:

$$\begin{aligned} \rho_{\text{qu}}(\mathbf{m}) &= \hat{Z}_{\text{qu}}^{-1}(\beta_{\text{qu}}) \prod_{\alpha=1,2} \exp\left[-\beta_{\text{qu}} \frac{Ca^2}{2} \sum_{\mathbf{j}} [\nabla m^\alpha(\mathbf{j}) - \mu^\alpha]^2\right]\ , \\ \hat{Z}_{\text{qu}}(\beta_{\text{qu}}) &= \prod_{\alpha=1,2} \sum_{\{m^\alpha(\mathbf{j})\}} \exp\left[-\beta_{\text{qu}} \frac{Ca^2}{2} \sum_{\mathbf{j}} [\nabla m^\alpha(\mathbf{j}) - \mu^\alpha]^2\right]\ , \end{aligned} \tag{52}$$

where μ^α is given by Eq. (18b). $\rho_{\text{qu}}(\mathbf{m})$ is the Gibbs state for a discrete Gaussian model, similar to those models used to study roughening transitions.[31] Remark: In Sec. II it was shown that for given λ, the only configurations that are metastable are those for which the fluctuations of the nearest-neighbor distances do not exceed a critical value. The fluid configurations we start with need not be metastable and the self-consistency condition (9) is generally not satisfied, as can be seen from (52): $\rho_{\text{qu}}(\mathbf{m})$ gives a nonzero probability to configurations with arbitrarily large fluctuations which are, therefore, not metastable. But our numerical investigations show that particles with $|u_0(\mathbf{j})| > a/2$ have negligible statistical weight in any configuration even for high quenching temperatures. This is clearly demonstrated by Fig. 6, where the distribution of the intracell positions is shown for a system with 22 particles.

Let us now turn to the calculation of the density of states. First we notice that ρ_{qu} splits up into two in-

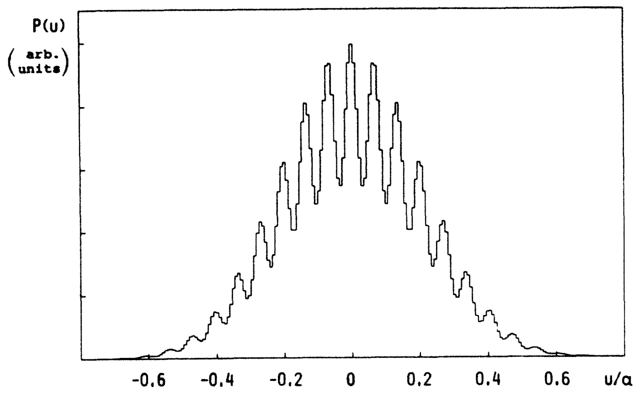

FIG. 6. The distribution $P(u)$ of the intracell positions $u(\mathbf{j})$ for $\lambda = 10$ and $k_B T_{\text{qu}}/(Ca^2/2) = 5$. $P(u)$ is given in arbitrary units. Particles with $|u(\mathbf{j})| \ge a/2$ violate the SCC.

dependent distributions for the spatial components. Consequently we will only consider one of these in the following and suppress α. Second, we introduce a slightly shorter notation which will turn out to be very convenient. Variables will be collected in N-dimensional vectors and summations over j will be denoted by scalar products:

$$x=\{x(\mathrm{j})\},\quad y=\{y(\mathrm{j})\}\ , \tag{53a}$$

$$x^T y=\sum_{\mathrm{j}} x(\mathrm{j})y(\mathrm{j})\ , \tag{53b}$$

$$x^2=x^T x\ . \tag{53c}$$

Thus, we can write the distribution (52) as

$$\begin{aligned} \rho_{\mathrm{qu}}(m)&=Z_{\mathrm{qu}}^{-1}(\beta_{\mathrm{qu}})\exp[-\beta(\nabla m-\mu)^2]\ ,\\ Z_{\mathrm{qu}}(\beta_{\mathrm{qu}})&=\sum_m \exp[-\beta(\nabla m-\mu)^2]\ , \end{aligned} \tag{54}$$

where we have set

$$\beta=\beta_{\mathrm{qu}}\frac{Ca^2}{2} \tag{55}$$

and $\sum_m=\sum_{\{m(\mathrm{j})\}}$. The asymmetries we have introduced in Sec. III are of the form

$$\varepsilon(0;m)=\varepsilon_0-\lambda Ca^2 g_\lambda^T \Delta m\ , \tag{56}$$

where $g_\lambda=\{g_\lambda(\mathrm{j})\}$.

Assuming the same self-averaging property as in Sec. IV the density of states is given by

$$\begin{aligned} n(\varepsilon)&=\langle\delta(\varepsilon-\varepsilon(0;m))\rangle_{\rho_{\mathrm{qu}}}\\ &=\frac{1}{2\pi}\int dt\, e^{it(\varepsilon-\varepsilon_0)}\langle e^{it\lambda Ca^2 g_\lambda^T\Delta m}\rangle_{\rho_{\mathrm{qu}}}\ . \end{aligned} \tag{57}$$

Now, averaging with respect to the distribution ρ_{qu} still requires determination of the boundary conditions for the configurations $\{m(\mathrm{j})\}$.[32] In order to avoid incommensurability effects, there remain two physically reasonable possibilities: (i) fixing the "volume" of the system at the most probable value or (ii) regarding the volume as one of the systems degrees of freedom. In Ref. 28 both possibilities are investigated in detail and shown to lead to the same results. Therefore, we will restrict ourselves to alternative (i), which is mathematically much easier to deal with. As μ is assumed to be integer valued we introduce new integer variables $m'(\mathrm{j})$ via

$$m(\mathrm{j})=\mu\cdot\mathrm{j}+m'(\mathrm{j})\ , \tag{58}$$

and impose periodic boundary conditions on $m'(\mathrm{j})$.

In order to calculate the expectation value in Eq. (57) we determine

$$\begin{aligned} f(\phi)&=\langle e^{i\phi^T\Delta m}\rangle_{\rho_{\mathrm{qu}}}\\ &=Z_{\mathrm{qu}}^{-1}\sum_m e^{-\beta(\nabla m-\mu)^2}e^{i\phi^T\Delta m}\ , \end{aligned} \tag{59}$$

where $\phi=\{\phi(\mathrm{j})\}$ is an arbitrary field with periodic boundary conditions. Because of $\nabla m-\mu=\nabla m'$, $\Delta m=\Delta m'$, and $\phi^T\Delta m'=(\Delta\phi)^T m'$, this can be transformed into

$$\begin{aligned} f(\phi)&=Z_{\mathrm{qu}}^{-1}\sum_{m'} e^{-\beta(\nabla m')^2}e^{i(\Delta\phi)^T m'}\\ &=Z_{\mathrm{qu}}^{-1}\sum_{m'} e^{\beta(\Delta m')^T m'}e^{i(\Delta\phi)^T m'}\ , \end{aligned} \tag{60a}$$

$$Z_{\mathrm{qu}}=\sum_{m'} e^{\beta(\Delta m')^T m'}\ . \tag{60b}$$

For mathematical convenience we replace the negative discrete Laplacian $-\Delta$ by $D_p=p-\Delta$ with a positive p and take the limit $p\rightarrow 0$ afterwards. This guarantees the existence of the inverse of the Laplacian and is equivalent to separating out the singular part of Δ. D_p is symmetric and positive definite, so there exists an operator B_p with $D_p=B_p^T B_p$. $f(\phi)$ can now be transformed into

$$\begin{aligned} f(\phi)&=Z_{\mathrm{qu}}^{-1}\sum_{m'} e^{-\beta(B_p m')^2}e^{-i(B_p\phi)^T(b_p m')}\ ,\\ Z_{\mathrm{qu}}&=\sum_{m'} e^{-\beta(B_p m')^2} \end{aligned} \tag{61}$$

As the summation over the discrete variables $m'(\mathrm{j})$ is not trivial the question arises: Can replacing the summations by integrations over continuous m' variables be regarded as a good approximation for high quenching temperature T_{qu}? An inspection of (61) shows that the answer is not at all clear. In the limit $\beta\rightarrow 0$, the first factor in the sum for $f(\phi)$ becomes a slowly varying function of m, whereas the second term does not. We will now calculate the density of states for continuous $m'(\mathrm{j})$ and show later that this is the right approximation for $\beta\rightarrow 0$ in a certain sense.

The details of the calculations can be omitted because the integrations are all Gaussian. We find

$$f_{\mathrm{cont}}(\phi)=\exp\left[-\frac{1}{4\beta}(B_p\phi)^2\right]\rightarrow\exp\left[-\frac{1}{4\beta}(\nabla\phi)^2\right]\quad \text{for } p\rightarrow 0\ , \tag{62}$$

which, inserted into (57), yields with the substitution $\phi=t\lambda Ca^2 g_\lambda$

$$\begin{aligned} n_{\mathrm{cont}}(\varepsilon)=&\left[\frac{\beta_{\mathrm{qu}}}{2\pi Ca^2\lambda^2\frac{\partial}{\partial\lambda}[\lambda g_\lambda(0)]}\right]^{1/2}\\ &\times\exp\left[-\frac{\beta_{\mathrm{qu}}(\varepsilon-\varepsilon_0)^2}{2Ca^2\lambda^2\frac{\partial}{\partial\lambda}[\lambda g_\lambda(0)]}\right]\ . \end{aligned} \tag{63}$$

Here we have used the identity (A5) for the Green's function. In this approximation the density of states is given by a Gauss function centered at $\varepsilon_0=-(Ca^2/2)\lambda g_\lambda(0)$ which is of the order of $Ca^2/2$ as can be seen from (A7). Using the same parameter values as in Sec. III we find that this function is practically constant on energy scales of 10^{-4} eV and smaller. This leads to a linear temperature dependence of the specific heat at temperatures below 1 K with a positive quadratic correction term.

Now the interesting question arises: Can the discreteness of the variables $m(\mathrm{j})$, which will become more prominent for lower quenching temperatures T_{qu}, modify this almost constant density of states? In particular, can it even produce a fine structure with self-similar properties as was found for the kink disorder in Sec. IV? To find an answer let us turn to the exact calculation of the density of states. To this end we apply the Poisson summation formula

$$\sum_{m=-\infty}^{\infty} \delta(x-m)=\sum_{n=-\infty}^{\infty} e^{2\pi i n x} \tag{64}$$

to Eq. (61). (This is a well-known procedure for related models, e.g., discrete Gaussian model, two-dimensional planar model, Villain model,[31] etc., resulting in a duality transformation which maps the high-temperature phase onto the low-temperature one and vice versa.) In our case the summation over $m'(\mathbf{j})$ will be converted into a summation over integer variables $n(\mathbf{j})$ [dual to $m'(\mathbf{j})$], which also obey periodic boundary conditions. After some algebra, the details of which are presented in Appendix C, we find

$$n(\varepsilon)=n_{\text{cont}}(\varepsilon)\frac{Z(\varepsilon-\varepsilon_0,\beta)}{N(\beta)}\ , \tag{65}$$

with

$$\begin{aligned} Z(\varepsilon,\beta)&=\sum_n{}' \exp\left[2\pi i\frac{n^T g_\lambda}{(\nabla g_\lambda)^2}\frac{\varepsilon}{\lambda C a^2}\right]\exp\left[-\frac{\pi^2}{\beta}n^T\left[\tilde{G}_0-\frac{g_\lambda g_\lambda^T}{(\nabla g_\lambda)^2}\right]n\right]\ ,\\ &=\sum_n{}' \cos\left[2\pi\frac{n^T g_\lambda}{(\nabla g_\lambda)^2}\frac{\varepsilon}{\lambda C a^2}\right]\exp\left[-\frac{\pi^2}{\beta}n^T\left[\tilde{G}_0-\frac{g_\lambda g_\lambda^T}{(\nabla g_\lambda)^2}\right]n\right]\ , \end{aligned} \tag{66a}$$

$$N(\beta)=\sum_n{}' \exp\left[-\frac{\pi^2}{\beta}n^T\tilde{G}_0 n\right]\ , \tag{66b}$$

where $\sum_n'$ means a restriction of the summation to those n with $\sum_{\mathbf{j}} n(\mathbf{j})=0$, $\tilde{G}_0$ stands for the matrix $\{\tilde{g}_0(\mathbf{j}-\mathbf{k})\}$, and $\tilde{g}_0$ denotes the lattice Green's function as described in Appendix A.

Thus, the full density of states is given by the continuum result multiplied with a "correction factor." This correction can be regarded as a superposition of oscillating terms (with respect to the energy ε), their relative weight given by an exponential of a quadratic form in n. To discuss these oscillations quantitatively several properties are crucial, and these are (for details see again Appendix C) given below.

(i) The quadratic form in the exponents of $Z(\varepsilon,\beta)$ is positive semidefinite and possesses a simple zero eigenvalue with corresponding direction $u=K\Delta g_\lambda$, where K is an arbitrary real constant. This direction is generically incommensurate with the integer vectors $n=\{n(\mathbf{j})\}$ (which form a lattice), i.e., this direction contains no other lattice point apart from zero.

(ii) Therefore, the main contribution to the correction factor stems from those n approximating the direction of u as well as possible. These n's can be grouped into "rays" (denoted by q) in n space. The problem is then converted to finding rays approximating the direction of u.

(iii) A special sequence of approximating rays, $[q^{(n)}]$, $n=1,2,\ldots$, is constructed from the representation of $g_\lambda(\mathbf{j})$ given in (A6a) under the assumption that λ is integer valued. (Although λ being an integer is necessary for the mathematical considerations of Appendix C, we believe the results to hold for general λ. This is supported by our numerical investigations.) The frequencies of the oscillating terms belonging to the $q^{(n)}$'s, $\omega^{(n)}$, are shown to form asymptotically a hierarchy,

$$\omega^{(n+1)}\approx\lambda\omega^{(n)} \text{ for } n\gg 1\ , \tag{67}$$

and to be integer multiples (up to corrections getting small with increasing n) of the basic frequency

$$\omega^{(1)}\approx 2\pi/(\varepsilon_0/2)\ . \tag{68}$$

It is argued that approximants not contained in the sequence will also lead to frequencies belonging to this hierarchy.

Thus it can be concluded that the correction factor gives rise to periodic modulations of the continuum result on any energy scale. Because of the existence of a basic frequency, cf. Eq. (68), the correction factor possesses maxima at energies $k\varepsilon_0/2$ (k integer), in particular at $\varepsilon=\varepsilon_0$. As a consequence, the density of states will always show a maximum at $\varepsilon=0$.

This is also supported by our numerical investigations. We have directly evaluated the density of states (DOS) via Eq. (57) for a system with 22 particles. The σ^α's varied from $\mu^\alpha-3$ to $\mu^\alpha+3$ which is reasonable for the range of quenching temperatures we have investigated. The modulations of the continuum result are clearly to be seen in Fig. 7 where the DOS is shown for increasing resolution on the energy axis. The hierarchical behavior already shows up although n is small there. Evaluating the exact recursion relation for the frequencies, (C22), gives a good quantitative agreement with those found in Fig. 7.

The last important point to be examined is the dependence of the correction factor on the quenching temperature T_{qu}. It can be easily seen from Eq. (C13) that the amplitude of the oscillating term belonging to q decreases with increasing T_{qu} for all q, thus leading to a "dying out" of frequencies. But the frequencies that die out first are those belonging to "bad" approximants, i.e., mainly to low frequencies. So, for a given energy scale, we will always find a crossover from a behavior dominated by the oscillations of the correction factor to an almost constant behavior of the density of states with increasing quench-

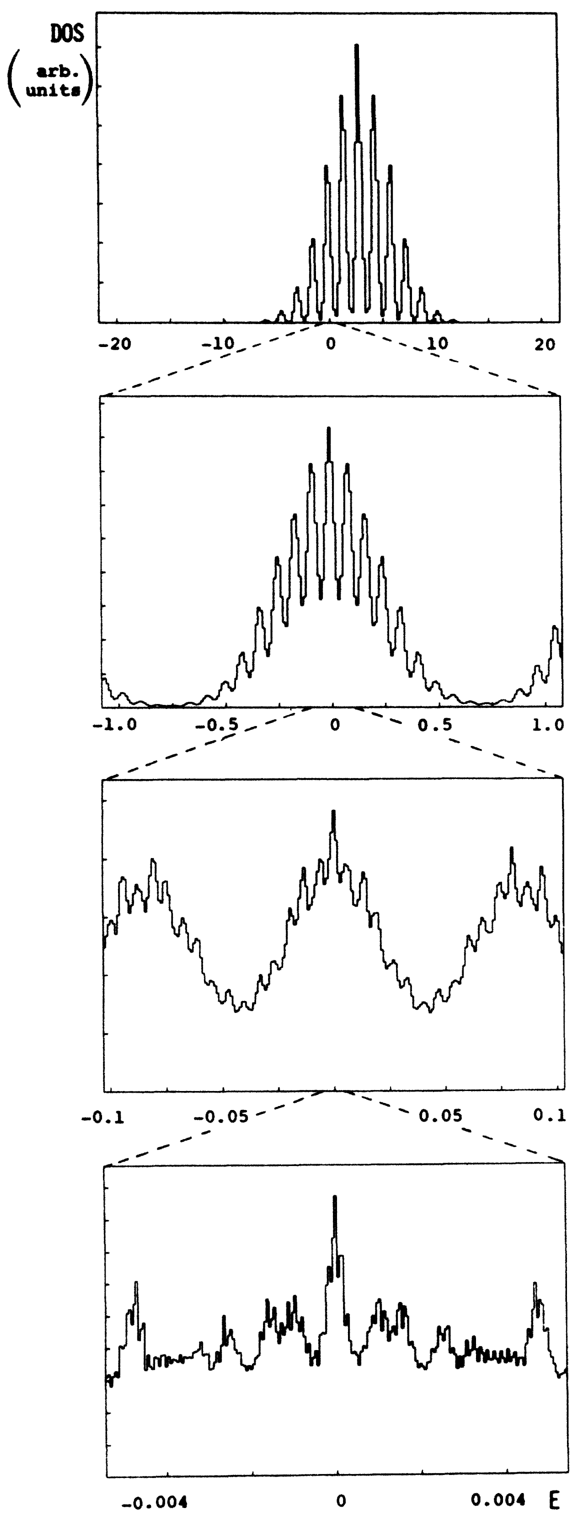

FIG. 7. The DOS for increasing resolution on the energy axis. The energy E is given in units of $Ca^2/2$ and the DOS in arbitrary units. The parameter values are $\lambda = 13.57$ and $k_B T_{qu}/(Ca^2/2) = 2$. The dashed lines indicate the part of the energy axis which is magnified on going one step from top to bottom.

ing temperature. This crossover occurs when the frequencies relevant for this energy scale just die out. Such a transition can be clearly seen in Fig. 8, where the energy scale is about $10^{-3}Ca^2/2$ and the quenching temperature varies in the interval $1 \le k_B T_{qu}/(Ca^2/2) \le 10$.

What are the consequences of these considerations for the low-temperature specific heat, i.e., for temperatures in the range 0.1–1 K corresponding to an energy scale of 10^{-4} eV and smaller? If the quenching temperature is sufficiently high or, equivalently, if the disorder is large enough, the specific heat will have a linear temperature dependence. (The numerical example shown in Fig. 8 reveals that quenching temperatures with $k_B T_{qu}$ in the order of 5–10 times the elastic energy of the adsorbate atoms are sufficient.) As the density of states always has a maximum at $\varepsilon = 0$ (stemming from the maximum of the correction factor at $\varepsilon = \varepsilon_0$), the first correction to the linear T law will be a negative T^3 term. This is in contrast to what results from the continuum approximation which would yield a positive T^2 term. For low quenching temperatures the density of states is dominated by the oscillations of the correction factor and looks rather bizarre. It is not clear whether a scaling behavior analogous to that of Sec. IV can be found. Thus, from the theoretical point of view, the interesting question remains open whether one can bridge the gap between Gaussian and kink disorder.

VI. DISCUSSION AND SUMMARY

In this paper we have investigated the metastable configurations of a two-dimensional Frenkel-Kontorova model in a regime for which the external potential is much larger than the harmonic nearest-neighbor coupling. The most natural realization of our model is an adsorbed layer of atoms on a substrate, but the application to quasi-two-dimensional ionic conductors, e.g., β-alumina, etc., may be reasonable, also. (The one-dimensional version was used to describe quasi-one-dimensional ionic conductors like hollandite with large success.[15,16,18,19])

As a first result we have found that the potential-energy landscape is rather complex; i.e., most of the metastable configurations are disordered. This is manifested by the fact that under certain conditions these configurations are in a one-to-one correspondence with sequences of symbols taking only integer values. Introducing the bond variables $\sigma(\mathbf{k})$, the one-to-one correspondence allows to interpret the disordered or glassy configurations as spatially chaotic arrangements of atoms analogous to the symbolic dynamics in dynamical systems exhibiting fully developed chaos. Moreover, this property demonstrates the applicability of the concept of spatial chaos to systems with more than one dimension (which correspond to dynamical systems with more than one time coordinate).

The exact knowledge of all the metastable configurations and of their energy turns out to be very important. In particular, we were able to derive the asymmetries, the potential barriers, the correlation between both, and the corresponding density of states $n(E)$

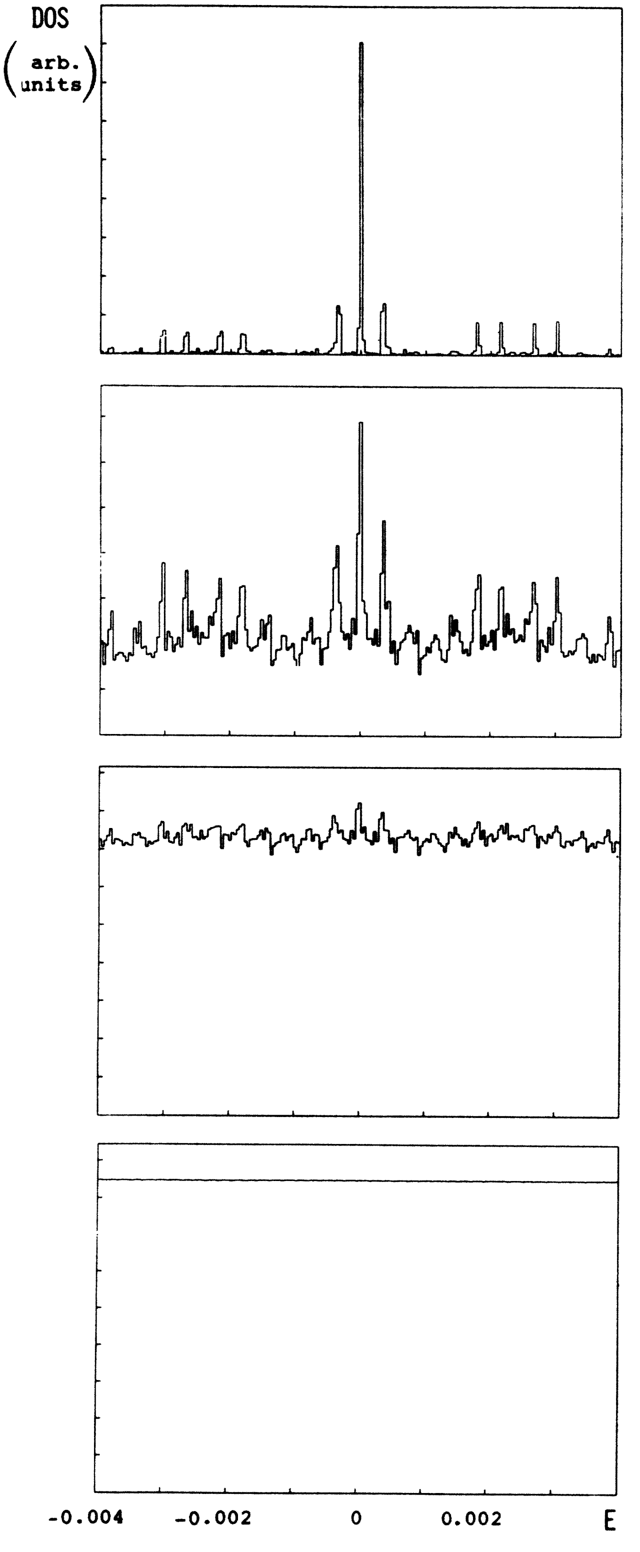

FIG. 8. The DOS for growing quenching temperature T_{qu} (from top to bottom) and low energy. The energy E is given in units of $Ca^2/2$ and the DOS in arbitrary units. β varies from top to bottom as 1.0,0.7,0.5,0.1; the relative strength of the substrate potential has the value $\lambda = 10$.

for the TLS's which are formed by configurational excitations. Here we have restricted ourselves to the simplest case where only one atom moves into one of its four adjacent cells. An intimate relationship between $n(E)$ and the distribution of the particle positions within the cell was found, which may lead to a connection between $n(E)$ and the pair distribution function $G(r)$. This point is under investigation.

One of the main results of the present work is the high sensitivity of $n(E)$ on the type and degree of disorder. For quasi-one-dimensional disorder, assuming "kink" defects, the one-dimensional behavior of Refs. 2 and 3 was reproduced leading for the specific heat to a power-law behavior $c(T) \sim T^{\tilde{d}}$ with a fractional exponent $\tilde{d}$ smaller than one. Quite a different kind of disorder results from an idealized quench process leading to "Gaussian disorder." Here the quenching temperature T_{qu} allows us to tune the degree of disorder. In case of large disorder, i.e., $k_B T_{\text{qu}}$ is large compared to the elastic energy $Ca^2/2$, we find an almost constant density of states (on an energy scale of 10^{-5}–10^{-4} eV, cf. Fig. 8) leading to a linear specific heat.

With decreasing T_{qu} $n(E)$ deviates more and more from a constant behavior and exhibits a rather bizarre behavior (Figs. 7 and 8) with more or less pronounced "gaps," quite similar to the results found by Pietronero and Strässler for the corresponding one-dimensional version of the model. However, the reader should note that our results are not just a two-dimensional generalization, the main difference being that we have considered metastable configurations with frozen-in disorder, whereas thermodynamical equilibrium states exhibiting incommensurability effects are studied there.

The "gap" structure appearing in $n(E)$ is a consequence of the discreteness of the variables $m(\mathbf{k})$. Since the dependence of physical quantities on discrete variables is characteristic for chaotic systems we may speculate that such a gap structure for the density of states may exist in general. Unfortunately, measuring average quantities, e.g., the specific heat, etc., cannot reveal these gaps unless they are very well pronounced. In other cases more direct methods to determine $n(E)$ would be necessary. It would also be helpful if $n(E)$ could be measured for E larger than 10^{-4} eV.

A further peculiarity of $n(E)$ occurs for Gaussian disorder: $n(E)$ is not symmetric with respect to $E = 0$ implying a nonvanishing Grüneisen parameter Γ_{TLS}.[33] This was found experimentally (although Γ_{TLS} was small) and as a possible explanation the asymmetry of $n(E)$ has been suggested.[33]

It is also tempting to speculate that the nondispersive excitations found by Lauter and co-workers[34] in absorbed helium films at 0.5 K could be interpreted as TLS. Indeed a fine structure was found for the corresponding density of states with a maximum at about 0.8 meV (cf. Fig. 8 of Ref. 34). But the resemblance of this experimental result and our $n(E)$ may be an accident.

Concerning the time dependence of $c(T)$ our model for a glassy adsorbed layer does not yield a logarithmic, but an exponential behavior due to a strong correlation between asymmetries and barrier heights of the TLS. As these two time laws can be well distinguished from each other, this prediction could probably be checked experimentally.

Finally we mention that we do not find a universal relationship between $n(0)$ (often called P) and the glass transition temperature T_g as it was deduced by Reichert *et al.*[35] This can be seen as follows: Taking the continuum result for $n(E)$ we get

$$n_{\text{cont}}(0)\sim(1/Ca^2)\exp(3\beta/\lambda^2)$$
$$\sim(\lambda/V)\exp[3\beta(Ca^2/V)^2] \ .$$

Here we have used that the barrier height $V\sim\lambda Ca^2$ for $\lambda\gg 1$. Assuming that $T_g\sim V$ (which is almost fixed for $\lambda\gg 1$), we find a relationship between $n_{\text{cont}}(0)$ and T_g depending on the elastic coupling constant C thereby ruling out such a universal relationship for our model. A similar conclusion was drawn by Berret and Meissner.[36]

Although the preparation of low-dimensional glassy systems is probably much more difficult than that of three-dimensional materials, it would be interesting to experimentally study the dependence of the properties of the TLS on the spatial dimension and particularly to check the predictions of our model for the density of states and the low-temperature specific heat. In addition, more systematical studies of the influence of the degree and type of disorder on the density of states could elucidate the origin and nature of the TLS.

ACKNOWLEDGMENTS

We would like to thank Dr. N. Theodorakopoulos for reading the manuscript. One of us (W.U.) is grateful for support from the Studienstiftung des deutschen Volkes. This work was supported in part by the Swiss National Science Foundation.

APPENDIX A: THE GREEN'S FUNCTION

According to Eq. (4) the Green's function g_λ belonging to the difference equation (2) is determined by

$$(D_\lambda g_\lambda)(\mathbf{k})=(\lambda+4)g_\lambda(\mathbf{k})-\sum_{\delta}g_\lambda(\mathbf{k}+\delta)=\delta_{\mathbf{k},0} \ . \quad \text{(A1)}$$

Using periodic boundary conditions we can solve this equation by Fourier transformation:

$$g_\lambda(\mathbf{k})=N^{-1}\sum_{\mathbf{q}}\exp(i\mathbf{q}\cdot\mathbf{k})/[\lambda+4-2(\cos q_1+\cos q_2)] \ , \quad \text{(A2)}$$

where the $\mathbf{q}$ summation runs over the first Brillouin zone.

1. General properties

Some properties of g_λ which can be easily deduced from Eq. (A1) are

$$\Delta g_\lambda(\mathbf{k})=\lambda g_\lambda(\mathbf{k})-\delta_{\mathbf{k},0} \ , \quad \text{(A3a)}$$

$$\sum_{\mathbf{k}}g_\lambda(\mathbf{k})=1/\lambda \ , \quad \text{(A3b)}$$

$$D_\mu g_\lambda(\mathbf{k})=\delta_{\mathbf{k},0}+(\mu-\lambda)g_\lambda(\mathbf{k}) \ . \quad \text{(A3c)}$$

Equation (A2) shows that $g_\lambda(\mathbf{k})$ only depends on $|k_1|$ and $|k_2|$. An expansion of the Green's function into a power series in $1/(\lambda+4)$ shows $g_\lambda(\mathbf{k})$ to be positive for all values of $\mathbf{k}$. Applying the difference operator D_λ to the expression $\sum_{\mathbf{j}}g_\mu(\mathbf{k}-\mathbf{j})g_\lambda(\mathbf{j})$ and using Eq. (A3c) yields

$$g_\lambda(\mathbf{k})-g_\mu(\mathbf{k})=-(\lambda-\mu)\sum_{\mathbf{j}}g_\lambda(\mathbf{k}-\mathbf{j})g_\mu(\mathbf{j}) \quad \text{(A4)}$$

which, upon division by $\lambda-\mu$ and $\mu\rightarrow\lambda$, is transformed into

$$\partial g_\lambda(\mathbf{k})/\partial\lambda=-\sum_{\mathbf{j}}g_\lambda(\mathbf{k}-\mathbf{j})g_\lambda(\mathbf{j}) \ . \quad \text{(A5)}$$

Expanding the right-hand side of (A2) into a power series of $1/\lambda$ (which is valid only for $\lambda>8$) yields

$$\lambda g_\lambda(\mathbf{k})=\sum_{l\geq 0}(1/\lambda)^l a_l(\mathbf{k}) \ , \quad \text{(A6a)}$$

where

$$a_l(\mathbf{k})=\Delta^l\delta_{\mathbf{k},0} \ , \quad \text{(A6b)}$$

from which it follows that

$$|a_l(\mathbf{j})|\leq 8^l \ , \quad \text{(A6c)}$$

$$a_l(\mathbf{j})=0 \quad \text{for} \quad |j_1|+|j_2|>l \ , \quad \text{(A6d)}$$

showing

$$\lambda g_\lambda(\mathbf{k})\rightarrow\delta_{\mathbf{k},0} \quad \text{for } \lambda\rightarrow\infty \ . \quad \text{(A7)}$$

Summing over one component of the double index $\mathbf{k}$ the Green's function of the one-dimensional version of our difference equation can be derived from (A2):

$$\sum_{k_2}g_\lambda(\mathbf{k})=N_1^{-1}\sum_{q_1}\exp(iq_1k_1)/(\lambda+2-2\cos q_1)$$
$$\rightarrow\frac{\eta}{1-\eta^2}\eta^{|k_1|} \quad \text{for } N_1\rightarrow\infty \ , \quad \text{(A8)}$$

where

$$\eta=1+\lambda/2-(\lambda+\lambda^2/4)^{1/2} \ .$$

2. Asymptotic behavior

In order to study the asymptotic behavior of the Green's function, which is needed in Sec. IV, we assume the expression for an infinite system to be a good approximation as long as $|k_\alpha|\ll N_\alpha$. Thus, we replace the summation in (A2) by an integration

$$N^{-1}\sum_{\mathbf{q}}\rightarrow(2\pi)^{-2}\int_{-\pi}^{\pi}\int_{-\pi}^{\pi}d^2\mathbf{q}$$

and use

$$1/(2D-\cos q_1-\cos q_2)$$
$$=\int_0^\infty dt\,\exp[-(2D-\cos q_1-\cos q_2)t] \ ,$$

where $D=1+\lambda/4$. Performing the integration over $\mathbf{q}$ leads to

$$g_\lambda(\mathbf{k})=\tfrac{1}{2}\int_0^\infty dt\,\exp(-2Dt)I_{|k_1|}(t)I_{|k_2|}(t)\,, \qquad \text{(A9)}$$

where I_μ is the modified Bessel function. Using the identity[33]

$$I_\mu(z)I_v(z)=(2/\pi)\int_0^{\pi/2} I_{\mu+v}(2z\cos\theta)\cos[(\mu-v)\theta]d\theta \quad [\mathrm{Re}(\mu+v)>-1] \qquad \text{(A10a)}$$

and[37]

$$\int_0^\infty \exp(-\alpha x)I_v(\beta x)dx=(\alpha^2-\beta^2)^{1/2}\beta^v[\alpha+(\alpha^2-\beta^2)^{1/2}]^{-v} \quad [\mathrm{Re}(v)>-1,\ \mathrm{Re}(\alpha)>|\mathrm{Re}(\beta)|\,]\,, \qquad \text{(A10b)}$$

one obtains

$$g_\lambda(\mathbf{k})=\frac{1}{2\pi}\int_0^{\pi/2}\frac{\cos^{\|\mathbf{k}\|_1}(\theta)\cos[(|k_1|-|k_2|)\theta]}{[D^2-\cos^2(\theta)]^{1/2}\{D+[D^2-\cos^2(\theta)]^{1/2}\}^{\|\mathbf{k}\|_1}}d\theta\,, \qquad \text{(A11)}$$

where $\|\mathbf{k}\|_1=|k_1|+|k_2|$. For $\|\mathbf{k}\|_1$ large, the factor $\cos^{\|\mathbf{k}\|_1}(\theta)$ will be significantly different from zero only for small θ. Consequently, the slowly varying parts of the integrand can be replaced by their values for $\theta=0$ which yields upon evaluating the integral

$$g_\lambda(\mathbf{k})\cong\tfrac{1}{4}(D^2-1)^{-1/2}\times[D+(D^2-1)^{1/2}]^{-\|\mathbf{k}\|_1}2^{-\|\mathbf{k}\|_1}\binom{\|\mathbf{k}\|_1}{|k_1|} \quad (\|\mathbf{k}\|_1\to\infty)\,. \qquad \text{(A12)}$$

This shows that the asymptotic behavior of $g_\lambda(\mathbf{k})$ is dominated by an exponentially decreasing factor. However, this decay is not isotropic, but shows a characteristic dependence on the direction reflecting the structure of the underlying square lattice: along the diagonals we find the slowest decrease.

3. The lattice Green's function

In Sec. V we need some properties of the Green's function belonging to the discrete Laplacian Δ. Consequently, we investigate the properties of the difference equation (A1) and its solution (A2) for $\lambda\to0^+$. Noticing that

$$g_\lambda(0)=N^{-1}\left[1/\lambda+\sum_{\mathbf{q}\neq0}1/[\lambda+4-2(\cos q_1+\cos q_2)]\right]\,, \qquad \text{(A13)}$$

it is obvious that $g_\lambda(0)$ diverges for $\lambda\to0$. To obtain the lattice Green's function this divergent term has to be substracted at any lattice point $\mathbf{k}$. Thus we consider the function

$$\tilde{g}_\lambda(\mathbf{k})=g_\lambda(\mathbf{k})-g_\lambda(0) \qquad \text{(A14)}$$

which has no divergency for $\lambda\to0$ as can be seen from (A2) and (A13). The following property holds for $\tilde{g}_0(\mathbf{k})$:

$$\sum_{\mathbf{k}}\tilde{g}_0(\mathbf{j}-\mathbf{k})\Delta x(\mathbf{k})=-x(\mathbf{j})+N^{-1}\sum_{\mathbf{k}}x(\mathbf{k})\,. \qquad \text{(A15a)}$$

This can be shown using (A3a),

$$\sum_{\mathbf{k}}\tilde{g}_\lambda(\mathbf{j}-\mathbf{k})\Delta x(\mathbf{k})=-x(\mathbf{j})+\sum_{\mathbf{k}}\lambda g_\lambda(\mathbf{j}-\mathbf{k})x(\mathbf{k})\,,$$

and (A2),

$$\lambda g_\lambda(\mathbf{j}-\mathbf{k})=N^{-1}\left[1+\sum_{\mathbf{q}\neq0}\lambda\exp[i\mathbf{q}\cdot(\mathbf{j}-\mathbf{k})]/[\lambda+4-2(\cos q_1+\cos q_2)]\right]\,.$$

Now for $\mathbf{q}\neq0$ we have

$$\lambda/[\lambda+4-2(\cos q_1+\cos q_2)] \le \max_\alpha \lambda/[\lambda+4-2\cos(2\pi/N_\alpha)]\to0$$

for $\lambda\to0$, implying

$$\lambda g_\lambda(\mathbf{j}-\mathbf{k})\to N^{-1} \quad \text{for } \lambda\to0\,.$$

Thus, for all x with $\sum_{\mathbf{k}}x(\mathbf{k})=0$,

$$\sum_{\mathbf{k}}\tilde{g}_0(\mathbf{j}-\mathbf{k})\Delta x(\mathbf{k})=-x(\mathbf{j}) \qquad \text{(A15b)}$$

is valid. This property is needed in Sec. V.

APPENDIX B: "EQUIVALENCE" OF SYMBOLS AND STATIONARY SOLUTIONS

Here we give a precise formulation of the equivalence of integer variables and stationary solutions of our system. This equivalence is fundamental for our considerations because it allows us to completely describe and characterize all solutions (in a certain class) of the difference equation (2)

$$(D_\lambda x_0)(\mathbf{j})=\lambda a m(\mathbf{j};x_0)\,, \qquad \text{(B1)}$$

where m and D_λ are defined in (1) and (3). As we have already seen, the solutions can be described by integer variables $\{m(\mathbf{j})\}$ provided the self-consistency condition

$$m(\mathbf{j})=\mathrm{int}[x_0(\mathbf{j};m)/a+\tfrac{1}{2}] \qquad \text{(B2a)}$$

or, equivalently,

$$\left|\sum_{\mathbf{k}}g_\lambda(\mathbf{j}-\mathbf{k})\Delta m(\mathbf{k})\right|<\tfrac{1}{2}\quad\forall\mathbf{j} \qquad \text{(B2b)}$$

is fulfilled. Here $x_0(\mathbf{j};m)$ is determined by

$$x_0(\mathbf{j};m)=am(\mathbf{j})+a\sum_{\mathbf{k}} g_\lambda(\mathbf{j}-\mathbf{k})\Delta m(\mathbf{k}) \ , \tag{B3}$$

and g_λ is the Green's function of D_λ. The reader should be careful not to confuse the set of integer variables $m=\{m(\mathbf{j})\}$ with the mapping $x_0 \mapsto m(x_0)=\{m(\mathbf{j};x_0)\}$.

The condition for the validity of (B2) and, therefore, for the correspondence between the integer configurations and the stationary configurations are stated in the following lemma: Let r be a positive number and let $\mathbf{l}(m)$ [for given $m=\{m(\mathbf{k})\}$] be determined by

$$\mathbf{l}(m)=N^{-1}\sum_{\mathbf{k}} \nabla m(\mathbf{k}) \ . \tag{B4}$$

Denote by M_r the set of m obeying

$$|d_\alpha m(\mathbf{j})-l^\alpha(m)| \le r \quad \forall \mathbf{j},\alpha \tag{B5}$$

and let X_r be the set of solutions x_0 of Eq. (B1) with

$$|d_\alpha m(\mathbf{j};x_0)-l^\alpha(m(x_0))| \le r \quad \forall \mathbf{j},\alpha \ . \tag{B6}$$

Then there exists a critical value $\lambda_c(r)>0$ such that the mapping $m \mapsto x_0(m)$ is one-to-one from M_r onto X_r for all $\lambda>\lambda_c(r)$.

To put this in other words: If the substrate potential is strong enough, then any set of integers $\{m(\mathbf{j})\}$ with bounded fluctuations of the "nearest-neighbor distances" [cf. Eq. (B5)] determines exactly one stationary solution with the same bounds for the fluctuations of the nearest-neighbor distances [cf. Eq. (B6)], and vice versa. $\mathbf{l}(m)$ is the mean value of the nearest-neighbor bonds around which the latter fluctuate. [Our considerations can be shown to be valid for any field $\mathbf{l}(\mathbf{j})$ with $\mathrm{div}\mathbf{l}(\mathbf{j})=0$. However, in order to fulfill the SCC $\mathbf{l}(m)$ turns out to be best.] That the strength λ of the substrate potential must exceed a critical value $\lambda_c(r)$ is required in order not to violate the self-consistency condition.

We split up the proof of the lemma into three parts: First, we show the existence of a $\lambda_c(r)$ such that for all $m\in M_r$ the self-consistency condition is satisfied provided $\lambda>\lambda_c(r)$. Assuming, then, the self-consistency condition to be satisfied, it is proved that $m\mapsto x_0(m)$ maps M_r onto X_r.[38] Finally, we show the mapping to be injective.

(i) Existence of $\lambda_c(r)$: We first notice, that $\mathbf{l}(m)$ is a constant field which implies $\mathrm{div}\mathbf{l}(m)=0$. Thus the SCC (B2) can be rewritten

$$\left|\sum_{\mathbf{k}} g_\lambda(\mathbf{j}-\mathbf{k})\mathrm{div}[\nabla m(\mathbf{k})-\mathbf{l}(m)]\right| < \tfrac{1}{2} \quad \forall \mathbf{j} \ .$$

With Eq. (A4b) we obtain

$$\left|\sum_{\mathbf{k}} g_\lambda(\mathbf{j}-\mathbf{k})\mathrm{div}[\nabla m(\mathbf{k})-\mathbf{l}(m)]\right| \le \max_{\mathbf{i}} |\mathrm{div}[\nabla m(\mathbf{i})-\mathbf{l}(m)]| \sum_{\mathbf{k}} g_\lambda(\mathbf{j}-\mathbf{k})$$
$$=(1/\lambda)\max_{\mathbf{i}} |\mathrm{div}[\nabla m(\mathbf{i})-\mathbf{l}(m)]| \ .$$

For $m\in M_r$ we have

$$\max_{\mathbf{i}} |\mathrm{div}[\nabla m(\mathbf{i})-\mathbf{l}(m)]| \le 4\max_{\mathbf{i},\alpha} |d_\alpha m(\mathbf{i})-l^\alpha(m)| \le 4r$$

according to Eq. (B5). Consequently the SCC is satisfied if $\lambda>8r$, this showing the existence of $\lambda_c(r)$ and giving an upper bound

$$\lambda_c(r)\le 8r \ . \tag{B7}$$

(ii) Surjectivity of the mapping: We now suppose the SCC to be satisfied and show that any $m\in M_r$ yields a $x_0\in X_r$ via the mapping (B3):

$$x_0(\mathbf{j})=am(\mathbf{j})+a\sum_{\mathbf{k}} g_\lambda(\mathbf{j}-\mathbf{k})\Delta m(\mathbf{k}) \ .$$

It follows that

$$\mathrm{int}[x_0(\mathbf{j})/a+\tfrac{1}{2}]=\mathrm{int}\left[m(\mathbf{j})+\sum_{\mathbf{k}} g_\lambda(\mathbf{j}-\mathbf{k})\Delta m(\mathbf{k})+\tfrac{1}{2}\right]$$
$$=m(\mathbf{j}) \ ,$$

and

$$\begin{aligned} u_0(\mathbf{j})&=x_0(\mathbf{j})-am(\mathbf{j};x_0)\\ &=x_0(\mathbf{j})-a\,\mathrm{int}[x_0(\mathbf{j})/a+\tfrac{1}{2}]\\ &=x_0(\mathbf{j})-am(\mathbf{j})\\ &=a\sum_{\mathbf{k}} g_\lambda(\mathbf{j}-\mathbf{k})\Delta m(\mathbf{k}) \ . \end{aligned}$$

Thus we have

$$(D_\lambda u_0)(\mathbf{j})=a\Delta m(\mathbf{j})$$

showing that x_0 is a solution of the difference equation (B1). That $x_0\in X_r$ follows directly from

$$m(\mathbf{j};x_0)=\mathrm{int}[x_0(\mathbf{j})/a+\tfrac{1}{2}]=m(\mathbf{j}) \ .$$

To show that the mapping $m\mapsto x_0(m)$ is onto X_r is trivial because any $x_0\in X_r$ determines a suitable $m\in M_r$ via the mapping $x_0\mapsto m(x_0)$.

(iii) Injectivity of the mapping: Let m be an element of M_r and suppose that there exist $x_0,x_0'\in X_r$ with

$$m(x_0)=m(x_0')=m \ . \tag{B8}$$

We set $y=x_0-x_0'$ and notice that

$$|y(\mathbf{j})|<a \quad \forall \mathbf{j}$$

according to (B8); i.e., $y(\mathbf{j})$ is bounded. Now, y is a solution of the linear equation

$$D_\lambda y(\mathbf{j})=(4+\lambda)y(\mathbf{j})-\sum_{\boldsymbol{\delta}} y(\mathbf{j}+\boldsymbol{\delta})=0 \ . \tag{B9}$$

Consider an arbitrary $\mathbf{j}_0$. According to (B9) there exists a nearest-neighbor $\mathbf{j}_0+\boldsymbol{\delta}_0$ with

$$|y(\mathbf{j}_0+\boldsymbol{\delta}_0)| \ge (1+\lambda/4)|y(\mathbf{j}_0)| \ .$$

Set $\mathbf{j}_1=\mathbf{j}_0+\boldsymbol{\delta}_0$ and go on with the procedure determining

δ_1, $\mathbf{j}_2$, etc. This yields a sequence $(\mathbf{j}_i)$, $i=0,1,2,\ldots$ with

$$|y(\mathbf{j}_i)| \geq (1+\lambda/4)^i |y(\mathbf{j}_0)| \ .$$

As $y(\mathbf{j})$ has been shown to be bounded this implies $y(\mathbf{j}_0)=0$. The proof is completed by noticing the arbitrariness of $\mathbf{j}_0$.

APPENDIX C: EFFECTS OF THE DISCRETENESS OF THE m's

In this appendix the technical details of Sec. V will be given, i.e., we investigate the effects of the discreteness of the variables $m(\mathbf{j})$.

1. Derivation of Eqs. (65) and (66)

After application of the Poisson summation formula (64) to Eq. (61) we get

$$\begin{aligned} f(\phi) &= Z_{\text{qu}}^{-1} \sum_n \int d^N x \, e^{-\beta(B_p x)^2} e^{-i(B_p\phi)^T(B_p x)} e^{2\pi i n^T x} \ , \\ Z_{\text{qu}} &= \sum_n \int d^N x \, e^{-\beta(B_p x)^2} e^{2\pi i n^T x} \ . \end{aligned} \tag{C1}$$

Let G_p be the inverse of D_p, i.e., G_p can be identified with the matrix $\{g_p(\mathbf{j}-\mathbf{k})\}$, cf. Eq. (4). Then we can write

$$n^T x = (D_p G_p n)^T x = (B_p G_p n)^T (B_p x) \ . \tag{C2}$$

Inserting (C2) into (C1) the x integrations can be carried out yielding

$$f(\phi) = \hat{Z}_{\text{qu}}^{-1} \sum_n \exp\left[-\frac{1}{4\beta}\phi^T D_p \phi\right] \exp\left[\frac{\pi}{\beta} n^T \phi\right] \times \exp\left[-\frac{\pi^2}{\beta} n^T G_p n\right] \ , \tag{C3a}$$

$$\hat{Z}_{\text{qu}} = \sum_n \exp\left[-\frac{\pi^2}{\beta} n^T G_p n\right] \ . \tag{C3b}$$

Now the limit $p \rightarrow 0$ can be performed without difficulty. The only thing one has to care about is the divergent part of G_p which must be subtracted:

$$\begin{aligned} n^T G_p n &= \sum_{\mathbf{k},l} n(\mathbf{k}) g_p(\mathbf{k}-l) n(l) \\ &= \sum_{\mathbf{k},l} n(\mathbf{k})[g_p(\mathbf{k}-l) - g_p(0)] n(l) + g_p(0) \left[\sum_l n(l)\right]^2 \\ &= \sum_{\mathbf{k},l} n(\mathbf{k}) \tilde{g}_p(\mathbf{k}-l) n(l) + g_p(0) \left[\sum_l n(l)\right]^2 \ . \end{aligned} \tag{C4}$$

In Appendix A it is shown that for $p \rightarrow 0$ $\tilde{g}_p$ just yields the lattice Green's function $\tilde{g}_0$, whereas $g_p(0) \rightarrow \infty$. Consequently

$$\exp\left[-\frac{\pi^2}{\beta} n^T G_p n\right] \underset{p\rightarrow 0}{\longrightarrow} \exp\left[-\frac{\pi^2}{\beta} n^T \tilde{G}_0 n\right] \delta_{\left[\sum_l n(l)\right],0} \tag{C5}$$

where δ denotes the Kronecker delta. Using this and

$$\phi^T D_p \phi \rightarrow -\phi^T \Delta \phi = (\nabla\phi)^2 \ , \tag{C6}$$

Eq. (C3) is changed into

$$\begin{aligned} f(\phi) &= Z_{\text{qu}}^{-1} {\sum_n}' \exp\left[-\frac{1}{4\beta}(\nabla\phi)^2\right] \exp\left[\frac{\pi}{\beta} n^T \phi\right] \\ &\quad \times \exp\left[-\frac{\pi^2}{\beta} n^T \tilde{G}_0 n\right] \ , \\ Z_{\text{qu}} &= {\sum_n}' \exp\left[-\frac{\pi^2}{\beta} n^T \tilde{G}_0 n\right] \ , \end{aligned} \tag{C7}$$

where $\sum_n'$ means a restriction of the summation to those n with $\sum_{\mathbf{j}} n(\mathbf{j})=0$. Replacing ϕ by $t\lambda C a^2 g_\lambda$ and inserting (C7) into (57), we finally get for the density of states the result given in Eqs. (65) and (66).

2. The zero eigenvalue of the quadratic form of the amplitudes

In the following we will be mainly interested in the energy dependence of the correction factor. As $N(\beta)$ is energy independent (it just accounts for the normalization of the DOS) we only have to examine $Z(\varepsilon,\beta)$.

As Eq. (66a) reveals, $Z(\varepsilon,\beta)$ consists of oscillating terms (with respect to the energy ε), their amplitude being determined by an exponential of a quadratic form in n. This quadratic form is positive semidefinite with a simple eigenvalue 0 that can be seen as follows: Let $\mathbf{v}$ be determined by

$$\mathbf{v} = \nabla \tilde{G}_0 n$$

which implies $\nabla^\dagger \cdot \mathbf{v} = n$. Then it is

$$n^T \left[\tilde{G}_0 - \frac{g_\lambda g_\lambda^T}{(\nabla g_\lambda)^2}\right] n = \mathbf{v}^T \cdot \left[1 - \frac{(\nabla g_\lambda)(\nabla g_\lambda)^T}{(\nabla g_\lambda)^2}\right] \cdot \mathbf{v} \geq 0 \tag{C8}$$

because the quadratic form for $\mathbf{v}$ consists of a projector with simple eigenvalue 0. Equation (C8) shows that the direction of the zero eigenvalue is given by $\mathbf{v} = K \nabla g_\lambda$ with an arbitrary real constant K. From the definition of $\mathbf{v}$ then it becomes clear that the direction of the zero eigenvalue is $u = -K \Delta g_\lambda$.

3. The approximation problem

Thus we have gained the following picture: The main contribution to the correction factor is given by those oscillating terms in the sum which have considerable weight. As we have seen in (C8) this means that only those n give a relevant contribution to $Z(\varepsilon,\beta)$ which approximate the "direction" of Δg_λ in n space. Now, the lattice formed by the variables $n=\{n(\mathbf{j})\}$ splits up into "rays" so that we can reduce the problem to finding rays approximating the Δg_λ direction. To be more precise, let

$$N = \left\{ n = \{n(\mathbf{j})\} \mid n(\mathbf{j}) \text{ integer}, \ \sum_{\mathbf{j}} n(\mathbf{j}) = 0 \right\} \tag{C9a}$$

and

$$Q=\{n\in N \mid \mathcal{G}(\{n(\mathbf{j})\})=1\}\ , \tag{C9b}$$

where $\mathcal{G}$ denotes the greatest common divisor. Any element $q\in Q$ now defines a "ray," and the summation over $n\in N$ of an arbitrary function f can be replaced by

$$\sum_{n\in N} f(n)=f(0)+\sum_{q\in Q}\sum_{r=1}^{\infty} f(rq)\ . \tag{C10}$$

Applying this formula to Eq. (66a) yields

$$Z(\varepsilon,\beta)=1+\sum_{q\in Q}\frac{1}{2}\left\{\Theta_3\left[\pi\frac{q^T g_\lambda}{(\nabla g_\lambda)^2}\frac{\varepsilon}{\lambda C a^2},\exp\left[-\frac{\pi^2}{\beta}q^T\left[\tilde{G}_0-\frac{g_\lambda g_\lambda^T}{(\nabla g_\lambda)^2}\right]q\right]\right]-1\right\}\ , \tag{C11}$$

which gives a splitting of the correction factor into the mean value and oscillating terms with zero mean and with frequency

$$\omega(q)=\frac{2\pi}{\lambda C a^2}\frac{q^T g_\lambda}{(\nabla g_\lambda)^2}\ . \tag{C12}$$

The summation in (C11) only runs over rays in n space. $\Theta_3(x,\gamma)$ denotes the Θ function as given in Ref. 39. It has period π with respect to x and its amplitude is determined by γ, i.e., the amplitudes of the oscillating terms in the correction factor depend on

$$a(q)=\exp\left[-\frac{\pi^2}{\beta}q^T\left[\tilde{G}_0-\frac{g_\lambda g_\lambda^T}{(\nabla g_\lambda)^2}\right]q\right]\ . \tag{C13}$$

Now we have to find rays approximating the direction of Δg_λ. If there existed a q having precisely this direction, this would imply

$$q(\mathbf{j})=K\Delta g_\lambda(\mathbf{j})\quad \forall \mathbf{j} \tag{C14a}$$

with a j-independent factor K. Equivalently we could write

$$q(\mathbf{j})=\frac{q(0)}{\Delta g_\lambda(0)}\Delta g_\lambda(\mathbf{j})\quad \forall \mathbf{j} \tag{C14b}$$

or

$$\frac{q(\mathbf{j})}{q(0)}=\frac{\Delta g_\lambda(\mathbf{j})}{\Delta g_\lambda(0)}\quad \forall \mathbf{j}\ . \tag{C14c}$$

As $q(\mathbf{j})/q(0)$ is a rational number, whereas the values of $\Delta g_\lambda(\mathbf{j})/\Delta g_\lambda(0)$ are generically not rational for all j, Eq. (C14c) does not hold. Thus we cannot find an integer valued q exactly in the direction of Δg_λ, but we can find q approximating this direction. As Eq. (C14c) reveals, this is equivalent to a simultaneous approximation of $N-1$ numbers by rationals.[40] A necessary condition for getting an ever closer approximation is $|q(\mathbf{j})|\to\infty$, $|q(0)|\to\infty$. Consequently we expect the existence of frequencies with nearly maximum amplitude belonging to some q with $q^2=\sum_{\mathbf{j}} q^2(\mathbf{j})$ and $|q(0)|$ large.

4. A special sequence of approximants

At first glance, things do not seem to have become a lot easier by transforming the summation in Eq. (66a) to rays. However, motivated by the representation (A6a) of the Green's function we will construct a special sequence of approximating rays, $[q^{(n)}]$, $n=1,2,\ldots$, which will permit some quantitative statements about the correction factor.

Following from (A6a) we have

$$\Delta g_\lambda(\mathbf{j})=\sum_{l=1}^{\infty}\left[\frac{1}{\lambda}\right]^l a_l(\mathbf{j})\ , \tag{C15a}$$

where [cf. Eq. (A6b)]

$$a_l(\mathbf{j})=\Delta^l\delta_{\mathbf{j},0} \tag{C15b}$$

is integer valued. Suppose now λ to be an integer [see the remark in Sec. V, (iii)]. An integer-valued approximant $q^{(n)}$ is then defined via

$$\begin{aligned} q^{(n)}(\mathbf{j})&=\lambda^n\sum_{l=1}^{n}\left[\frac{1}{\lambda}\right]^l a_l(\mathbf{j})\\ &=\sum_{l=1}^{n}\lambda^{n-l}a_l(\mathbf{j})\quad (n=1,2,\ldots)\ . \end{aligned} \tag{C16}$$

In (A6c) $a_l(\mathbf{j})$ has been estimated:

$$|a_l(\mathbf{j})|\le 8^l\quad \forall \mathbf{j} \tag{C17}$$

yielding

$$\frac{q^{(n)}(\mathbf{j})}{q^{(n)}(0)}=\frac{\Delta g_\lambda(\mathbf{j})}{\Delta g_\lambda(0)}+O\left[\left[\frac{8}{\lambda}\right]^{n+1}\right] \tag{C18}$$

which shows the required approximation property. (The quality of the approximation still depends on j.)

We, furthermore, have to show that the $q^{(n)}$ belong to the set of "rays," Q. From (A6b) and (A6d) it can be deduced that $a_n(\pm n\mathbf{e}_\alpha)=1$, $\alpha=1,2$ (provided $N_\alpha>2n$) showing that $\mathcal{G}(\{q^{(n)}(\mathbf{j})\})=1$. Thus $q^{(n)}\in Q$.

In order to study the asymptotic behavior of the frequencies $\omega(q^{(n)})$ (for large n) we give a recursion relation for the $q^{(n)}$ following from (C16) and (C15b):

$$q^{(n+1)}(\mathbf{j})=\Delta[q^{(n)}(\mathbf{j})+\lambda^n\delta_{\mathbf{j},0}]\ . \tag{C19}$$

The obvious symmetries of $q^{(n)}(\mathbf{j})$ with respect to j show that the values of the approximants at $\mathbf{j}=0$ (which will turn out to be important) contain a factor 4 for all n:

$$q^{(n+1)}(0)=4[q^{(n)}(\mathbf{e}_1)-q^{(n)}(0)+\lambda^n]\ . \tag{C20}$$

Now, the most interesting question is: What are the frequencies belonging to the $q^{(n)}$? Inserting (C16) into

(C11) and using (C18) we find

$$\omega^{(n)} \equiv \omega(q^{(n)}) = \frac{2\pi}{\varepsilon_0/2} \frac{q^{(n)}(0)}{4} \left[1 + O\left[\left| \frac{8}{\lambda} \right|^{n+1} \right] \right] , \tag{C21a}$$

where ε_0 is given by Eq. (20b). Thus we have approximately

$$\omega^{(n)} \approx \frac{2\pi}{\varepsilon_0/2} \frac{q^{(n)}(0)}{4} \tag{C21b}$$

showing that all frequencies are integer multiples of the basic frequency $\omega^{(1)} \approx 2\pi/(\varepsilon_0/2)$ (up to corrections getting small for increasing n). As a consequence the correction factor possesses maxima at energies $k\varepsilon_0/2$ (k integer). This is clearly revealed by the top part of Fig. 7 (lowest energy resolution) where the oscillation with $\omega^{(1)}$ can be seen. Because of the presence of $\omega^{(1)}$ the density of states will always show a maximum at $\varepsilon = 0$.

To investigate the asymptotic behavior of the frequencies $\omega^{(n)}$ ($n \gg 1$) we consider the recursion relation following from Eqs. (C11) and (C19):

$$\omega^{(n+1)} = \lambda \omega^{(n)} - \frac{2\pi}{\lambda C a^2} \frac{q^{(n)}(0) - \lambda^n \Delta g_\lambda(0)}{(\nabla g_\lambda)^2} , \tag{C22}$$

where we have used (A3a). From Eq. (C16) we deduce that the second term on the right-hand side (rhs) becomes negligible compared to first term for large n:

$$\omega^{(n+1)} \approx \lambda \omega^{(n)} \text{ for } n \gg 1 . \tag{C23}$$

Asymptotically this yields a hierarchy of frequencies that is already indicated in Fig. 7. (The way Figs. 7 and 8 were obtained is described in Sec. V.)

Up to now we have only considered a special sequence of integer approximants to the Δg_λ direction. What can be said about the other q in the sum of Eq. (C10)? We conjecture that for any approximant q there must exist a $q^{(n)}$ differing from q only for j's with $|j_1| + |j_2|$ in the order of, or larger than, n because otherwise q would not be a good approximant. But as the frequency is mainly determined by $q^{(n)}(0)$, this q will lead to an oscillating term with a frequency in the vicinity of $\omega^{(n)}$. Thus it can be concluded that asymptotically the hierarchical behavior of the frequencies still holds even in the case that all $q \in Q$ in the sum are considered.

---

[1] P. Reichert and R. Schilling, Phys. Rev. B **30**, 917 (1984).

[2] R. Schilling, Phys. Rev. Lett. **53**, 2258 (1984).

[3] P. Reichert and R. Schilling, Phys. Rev. B **32**, 5731 (1985).

[4] P. W. Anderson, B. I. Halperin, and C. M. Varma, Philos. Mag. **25**, 1 (1972).

[5] W. A. Phillips, J. Low Temp. Phys. **7**, 351 (1972).

[6] R. C. Zeller and R. O. Pohl, Phys. Rev. B **4**, 2029 (1971).

[7] J. C. Lasjaunias, A. Ravex, M. Vandorpe, and S. Hunklinger, Solid State Commun. **17**, 1045 (1975); J. C. Lasjaunias and A. Ravex, J. Phys. F **13**, L101 (1983); A. Ravex, J. C. Lasjaunias, and O. Bethoux, Physica B+C **107B**, 397 (1981).

[8] M. Meissner and K. Spitzmann, Phys. Rev. Lett. **46**, 265 (1981).

[9] L. W. Molenkamp and D. A. Wiersma, J. Chem. Phys. **83**, 1 (1985).

[10] *Amorphous Solids: Low Temperature Properties,* edited by W. A. Phillips (Springer-Verlag, Berlin, 1981).

[11] H. v. Löhneysen, Phys. Rep. **79**, 161 (1981).

[12] S. Hunklinger and A. K. Raychaudhuri, in *Progress in Low Temperature Physics,* edited by D. F. Brewer (Elsevier, Amsterdam, 1986), Vol. IV.

[13] R. N. Barnett, C. L. Cleveland, and U. Landman, Phys. Rev. Lett. **55**, 2035 (1985).

[14] F. C. Frank and J. H. van der Merwe, Proc. R. Soc. London Ser. A **198**, 205 (1949); **198**, 216 (1949); J. Frenkel and T. Kontorova, J. Phys. (Moscow) **1**, 337 (1939).

[15] S. Aubry, in *Solitous and Condensed Matter Physics,* edited by A. R. Bishop and T. Schneider (Springer, Berlin, 1978); J. Phys. C **16**, 2497 (1983); F. Vallet, R. Schilling, and S. Aubry, Europhys. Lett. **2**, 815 (1986).

[16] L. Pietronero and S. Strässler, Phys. Rev. Lett. **42**, 188 (1979).

[17] V. I. Arnold and A. Avez, *Ergodic Problems in Classical Mechanics* (Benjamin, New York, 1968).

[18] H. U. Beyeler, L. Pietronero, and S. Strässler; Phys. Rev. B **22**, 2988 (1980); L. Pietronero, W. R. Schneider, and S. Strässler, *ibid.* **24**, 2187 (1981).

[19] H. von Löhneysen, H. J. Schink, W. Arnold, H. U. Beyeler, L. Pietronero, and S. Strässler, Phys. Rev. Lett. **46**, 1213 (1981).

[20] G. Ertl (private communication).

[21] J. Jäckle, Z. Phys. **257**, 212 (1972).

[22] In general one has to add the difference of the zero-point energies for both metastable configurations to ε. For our model this does not depend on the configuration and therefore drops out.

[23] In order not to confuse the tunneling parameter with the relative strength of the substrate potential we use Λ instead of the common λ.

[24] Assuming that only the polarizations along the surface contribute to the deformation potential gives a reduction of Jäckle's result by a factor $\frac{2}{3}$. As the bulk material is only located at one side of the surface an additional factor $\frac{1}{2}$ must be accounted for.

[25] Up to now the only restriction for the configurations has been (14) which was required to fulfill the self-consistency condition. But from a physical point of view it is unreasonable to consider configurations violating the "regularity" of the $m(\mathbf{j})$'s. For example, we have to dismiss configurations where, e.g., the "right" nearest-neighbor, $\mathbf{j}+\mathbf{e}_1$, of a particle $\mathbf{j}$ is sitting on the left side of this particle. However, such configurations are already excluded by (14) if we choose $0 < r \leq l^\alpha$. As in the following $l^\alpha = \mu^\alpha$, and since we will only consider ρ which gives zero or negligible weight to configurations not fulfilling the SCC (14), this only gives a restriction for the fluctuations of the nearest-neighbor bonds, r, compared to the equilibrium length μ^α of the bonds.

[26] Here we have assumed that averages over all particles $\mathbf{j}_0$ can be replaced by fixing $\mathbf{j}_0$ and averaging over all configurations. This corresponds to the assumption of self-averaging or "ergodicity," see, e.g., J. M. Ziman, *Models of Disorder* (Cambridge, England, 1979).

[27] P. S. Lomdahl and D. J. Srolovitz, Phys. Rev. Lett. **57**, 2702

(1986); D. J. Srolovitz and P. S. Lomdahl, Physica D **23**, 402 (1986).

[28] W. Uhler, Ph.D. thesis, University of Basel, 1988.

[29] Because $\eta \approx 0.16$ the gaps in $n(E)$ are rather large (cf. Fig. 1 in Ref. 2). Therefore, the power law will be modulated by a Schottky-type behavior. This modulation is negligible only for $\eta > 0.2$.

[30] Note the difference to integrating out the vibrational degrees of freedom. This would yield a distribution function $\rho \sim \exp[-\beta_{\mathrm{qu}} E(m)]$ where $E(m)$ is given by (17) substituting (18a).

[31] J. Villain, J. Phys. (Paris) **36**, 581 (1975); S. D. Chui and J. D. Weeks, Phys. Rev. B **14**, 4978 (1976); J. V. Jose, L. P. Kadanoff, S. Kirkpatrick, and D. R. Nelson, Phys. Rev. B **16**, 1217 (1977); R. Savit, Phys. Rev. B **17**, 1340 (1978).

[32] In Sec. II we assumed periodic boundary conditions for the intracell positions $u(\mathbf{j})$ which has no influence on the boundary conditions for $m(\mathbf{j})$.

[33] A. C. Anderson, Phys. Rev. B **34**, 1317 (1986).

[34] H. J. Lauter, H. Godfrin, C. Tiby, H. Wiechert, and P. E. Obermayer, Surf. Sci. **125**, 265 (1983).

[35] U. Reichert, M. Schmidt, and S. Hunklinger, Solid State Commun. **57**, 315 (1986).

[36] J. F. Berret and M. Meissner, Z. Phys. B **70**, 65 (1988).

[37] *Table of Integrals, Series, and Products,* edited by I. S. Gradshteyn and I. M. Ryzhik (Academic, New York, 1980).

[38] It can even be shown that the surjectivity of the mapping is equivalent to the fulfillment of the self-consistency condition.

[39] E. T. Whittaker and G. N. Watson, *Modern Analysis* (Cambridge, England, 1946).

[40] I. Niven, *Irrational Numbers,* No. 11 of *The Carus Mathematical Monographs* (Wiley, New York, 1956).